Eur. Phys. J. C (2021) 81:813
https://doi.org/10.1140/epjc/s10052-021-09583-x

THE EUROPEAN PHYSICAL JOURNAL C

Regular Article - Theoretical Physics

Physical constraints derived from FCNC in the 3-3-1-1 model

Duy Nguyen Tuan[1,2,a], **Takeo Inami**[1,3], **Huong Do Thi**[1,b]

[1] Institute of Physics, VAST, 10 Dao Tan, Ba Dinh, Hanoi, Vietnam
[2] Graduate University of Science and Technology, Vietnam Academy of Science and Technology, 18 Hoang Quoc Viet, Cau Giay, Hanoi, Vietnam
[3] Theoretical Research Division, Nishina Center, RIKEN, Wako 351-0198, Japan

Received: 8 February 2021 / Accepted: 28 August 2021 / Published online: 14 September 2021

Abstract We investigate several phenomena related to FCNCs in the 3-3-1-1 model. The sources of FCNCs at the tree-level from both the gauge and Higgs sectors are clarified. Experiments on the oscillation of mesons most stringently constrain the tree-level FCNCs. The lower bound on the new physics scale is imposed more tightly than in the previous, $M_{new} > 12$ TeV. Under this bound, the tree-level FCNCs make a negligible contribution to the $Br(B_s \to \mu^+\mu^-)$, $Br(B \to K^*\mu^+\mu^-)$ and $Br(B^+ \to K^+\mu^+\mu^-)$. The branching ratio of radiative decay $b \to s\gamma$ is enhanced by the ratio $\frac{v}{u}$ via diagrams with the charged Higgs mediation. In contrast, the charged currents of new gauge bosons significantly contribute to the decay process $\mu \to e\gamma$.

1 Introduction

The analysis of phenomena related to flavor-changing neutral currents (FCNCs) plays an important role in constraining the parameters of the Standard Model (SM) and testing physics beyond the standard model (BSM). In recent years, the most extensively studied processes related to FCNCs in B-physics, particularly the exclusive $b \to s$ transition. The first place to look for new physics (NP) in $b \to s$ transitions is $B_q - \bar{B}_q$ mixing with $q = d, s$. The mass splitting ΔM_d has been measured with high precision [1], whereas the measurement of ΔM_s [2,3] is complicated because of the rapid oscillation of B_s meson. The measurement results of $Br(B_s \to \mu^+\mu^-)$ [4–7], $Br(b \to s\gamma)$ [8–11], are almost in agreement with the SM predictions. However, some small tensions related to the above processes have been persisted and confirmed by independent measurements. These tensions can be understood due to uncertainties of the form factors, CKM elements, or by the presence of NP. Moreover, the ratios of branching fractions R_K, R_{K^*}, and several observables of the $B \to K(K^*)l^+l^-$ $(l = \mu, e)$ decays have been determined [12–24]. All the results of these measurements have confirmed the deviation from the predictions of the SM. Unlike the angular observables, the various ratios of branching fractions can not be explained via underestimating hadron effects. This result has inspired physicists to investigate these decay processes and see whether some NP models can better explain the experimental data.

Recently, Dong and his collaborators have pointed out the simple extension of the SM in which the gauge symmetry has been extended to the $SU(3)_C \times SU(3)_L \times U(1)_X \times U(1)_N$ group, referred to as the 3-3-1-1 model. This model contains both mathematical and phenomenological aspects of the 3-3-1 model [25–30]. Therefore, the 3-3-1-1 model has all the good features of the 3-3-1 models [31–34]. The difference between the 3-3-1-1 model and previous 3-3-1 versions is the nature of $B - L$ symmetry . In the 3-3-1-1 model, the $B - L$ symmetry is known as a non-commutative gauge symmetry. Therefore, there exists a unification between the electroweak and $B - L$ interactions [35], which is similar to the Glashow-Weinberg-Salam theory. In addition, the model also provides a natural, comprehensive scenario to account for neutrino masses, dark matter, inflation, and leptogenesis [35].

Another feature of the 3-3-1-1 model is that flavor-violating interactions appear in both the quark and lepton sectors. The quark families transform differently under $SU(3)_L$. So, they lead to tree-level flavor-changing neutral currents (FCNCs) that couple to the new neutral gauge bosons, Z_2, Z_N, and the new neutral Higgs bosons. The role of FCNCs coupled to Z_2, Z_N in the oscillation of mesons has been studied in [32,36]. The authors only focused on the NP short-distance tree-level contribution caused by new neutral gauge bosons to the mass difference of mesons in those studies. The authors used only the NP contributions to compare with the experimental values. Thus, they have pointed out the lower bound on the NP scale in the TeVs. However,

[a] e-mail: ntdem@iop.vast.ac.vn (corresponding author)
[b] e-mail: dthuong@iop.vast.ac.vn

considering all NP and SM contributions to the meson oscillations, the lower bound may be more constrained than the previously known ones [32,36].

In this paper, we study all tree-level FCNCs associated with both Higgs and gauge bosons. The contributions coming from the FCNCs combined with these of SM are subject to strong constraints from meson mixing parameters. Phenomenological aspects related to FCNCs at tree-level, namely $B_s \to \mu^+\mu^-$, $B \to K^*\mu^+\mu^-$ and $B^+ \to K^+\mu^+\mu^-$ decays are expensive goals. Additionally, the 3-3-1-1 model predicts the existence of new charged particles, such as new non-Hermitian gauge bosons $Y^{\pm}_{\mu}$, the charged Higgs bosons $H^{\pm}_{4,5}$. They couple to both SM quarks, leptons to new heavy quarks, leptons, respectively. These interactions are the source for yielding the charged lepton flavor violation (LFV) processes $l_i \to l_j\gamma$ and $b \to s\gamma$ decay.

We organize our paper as follows. In Sect. 2, we briefly overview the 3-3-1-1 model. In Sect. 3, we describe the tree-level FCNCs and study their effects on the mass difference of mesons. We predict the NP contributions to the rare decays of $B_s \to \mu^+\mu^-$, $B \to K^*\mu^+\mu^-$ and $B^+ \to K^+\mu^+\mu^-$ processes based on the constrained parameter space. Section 4 studies the one-loop calculation of the relevant Feynman diagrams, which relate to the $b \to s\gamma$ and $\mu \to e\gamma$. The consequences of the parameters on the branching ratio of these decays are implied from the experimental data studied. Our conclusions are given in Sect. 5.

2 A summary of the 3-3-1-1 model

2.1 Symmetry and particle content

The gauge symmetry of the model is $SU(3)_C \times SU(3)_L \times U(1)_X \times U(1)_N$, where $SU(3)_C$ is the color group, $SU(3)_L$ is an extension of the $SU(2)_L$ weak-isospin, and $U(1)_X$, $U(1)_N$ define the electric charge Q and $B-L$ operators [36] as follows

$$Q = T_3 + \beta T_8 + X, \quad B - L = \beta' T_8 + N, \tag{1}$$

where β, β' are coefficients, and both are free from anomalies. The parameters β, β' determine the Q and $B-L$ charges of new particles. In this work, we consider the model with $\beta = -\frac{1}{\sqrt{3}}$. This is the simple 3-3-1-1 model for dark matter [31]. The leptons and quarks, free of all gauge anomalies, transform as

$$\begin{aligned}
&\psi_{aL} = (\nu_{aL}, e_{aL}, (N_{aR})^c)^T \sim (1, 3, -1/3, -2/3),\\
&\nu_{aR} \sim (1, 1, 0, -1), \quad e_{aR} \sim (1, 1, -1, -1),\\
&Q_{\alpha L} = (d_{\alpha L}, -u_{\alpha L}, D_{\alpha L})^T \sim (3, 3^*, 0, 0),\\
&Q_{3L} = (u_{3L}, d_{3L}, U_L)^T \sim (3, 3, 1/3, 2/3),\\
&u_{aR} \sim (3, 1, 2/3, 1/3), \quad d_{aR} \sim (3, 1, -1/3, 1/3),\\
&U_R \sim (3, 1, 2/3, 4/3), \quad D_{aR} \sim (3, 1, -1/3, -2/3),
\end{aligned} \tag{2}$$

where $a = 1, 2, 3$, $\alpha = 1, 2$ are the generation indexes. The scalar sector, which is necessary for realistic symmetry breaking and mass generation, consists of the following Higgs fields [31]

$$\begin{aligned}
\eta^T &= (\eta_1^0, \eta_2^-, \eta_3^0)^T \sim (1, 3, -1/3, 1/3),\\
\rho^T &= (\rho_1^+, \rho_2^0, \rho_3^+)^T \sim (1, 3, 2/3, 1/3),\\
\chi^T &= (\chi_1^0, \chi_2^-, \chi_3^0)^T \sim (1, 3, -1/3, -2/3),\\
\phi &\sim (1, 1, 0, 2).
\end{aligned} \tag{3}$$

The electrically-neutral scalars can develop vacuum expectation values (VEVs)

$$\begin{aligned}
&<\eta_1^0> = \frac{u}{\sqrt{2}}, \quad <\rho_2^0> = \frac{v}{\sqrt{2}},\\
&<\chi_3^0> = \frac{w}{\sqrt{2}}, \quad <\phi> = \frac{\Lambda}{\sqrt{2}},
\end{aligned} \tag{4}$$

and break the symmetry of model via the following scheme

$$\begin{aligned}
&SU(3)_C \otimes SU(3)_L \otimes U(1)_X \otimes U(1)_N\\
&\downarrow \Lambda\\
&SU(3)_C \otimes SU(3)_L \otimes U(1)_X \otimes P\\
&\downarrow w\\
&SU(3)_C \otimes SU(2)_L \otimes U(1)_{B-L} \otimes P\\
&\downarrow u, v\\
&SU(3)_C \otimes U(1)_Q \otimes P,
\end{aligned}$$

where P is understood as the matter parity (W-parity) and takes the form: $P = (-1)^{3(B-L)+2s}$. All SM particles have W-parity of $+1$ (called even W-particle) while new fermions have W-parity of -1 (called odd W-particle). With W-parity preserved, the lightest odd W-particle can not decay. If the lightest particle has a neutral charge, it may account for dark matter (see [31]). The VEVs, u, v, break the electroweak symmetry and generate the mass for SM particles with the consistent condition: $u^2 + v^2 = 246^2$ GeV^2. The VEVs, w, Λ, break $SU(3)_L$, $U(1)_N$ groups and generate the mass for new particles. For consistency, we assume $w, \Lambda \gg u, v$.

2.2 Scalar sector

Let us rewrite the scalar potential [32,33] that consists of three terms, $V = V(\phi) + V(\eta, \rho, \chi) + V_{\text{mix}}$, where

$$\begin{aligned}
V(\phi) &= \mu_\phi^2 \phi^\dagger\phi + \lambda(\phi^\dagger\phi)^2,\\
V(\eta, \chi, \rho) &= \mu_1^2 \rho^\dagger\rho + \mu_2^2 \chi^\dagger\chi + \mu_3^2 \eta^\dagger\eta\\
&\quad + \lambda_1(\rho^\dagger\rho)^2 + \lambda_2(\chi^\dagger\chi)^2 + \lambda_3(\eta^\dagger\eta)^2,\\
V_{\text{mix}} &= \lambda_4(\rho^\dagger\rho)(\chi^\dagger\chi) + \lambda_5(\rho^\dagger\rho)(\eta^\dagger\eta)\\
&\quad + \lambda_6(\chi^\dagger\chi)(\eta^\dagger\eta) + \lambda_7(\rho^\dagger\chi)(\chi^\dagger\rho)\\
&\quad + \lambda_8(\rho^\dagger\eta)(\eta^\dagger\rho) + \lambda_9(\chi^\dagger\eta)(\eta^\dagger\chi)\\
&\quad + \lambda_{10}(\phi^\dagger\phi)(\rho^\dagger\rho) + \lambda_{11}(\phi^\dagger\phi)(\chi^\dagger\chi)
\end{aligned}$$

$$+(f\epsilon^{mnp}\eta_m\rho_n\chi_p + H.c.). \quad (5)$$

Due to the W-parity conservation, only neutral scalar fields carrying W-parity of +1 can develop VEV. After symmetry breaking, there is no mixing between the even and odd W-fields (see in [33]). For the even W-particle spectrum, the model has predicted

- Four neutral physical particles with CP-even, one identified as the SM-like Higgs boson H and the three remaining particles, H_i, $i = 1, 2, 3$, are new heavy fields, having the following form

$$\begin{aligned} H &= \frac{u\Re(\eta_1^0) + v\Re(\rho_2^0)}{\sqrt{u^2+v^2}}, \\ H_1 &= \frac{-v\Re(\eta_1^0) + u\Re(\rho_2^0)}{\sqrt{u^2+v^2}}, \\ H_2 &= \cos\varphi\Re(\chi_3) + \sin\varphi\Re(\phi), \\ H_3 &= -\sin\varphi\Re(\chi_3) + \cos\varphi\Re(\phi), \end{aligned} \quad (6)$$

  where $\tan(2\varphi) = -\frac{\lambda_{11}w\Lambda}{\lambda\Lambda^2-\lambda_2 w^2}$.
- One neutral CP-odd particle

$$\mathcal{A} \simeq \frac{v\Im(\eta_1) + u\Im(\rho_2)}{\sqrt{u^2+v^2}}. \quad (7)$$

- Two charged fields that are given as follows

$$H_4^{\pm} = \frac{v\chi_2^{\pm} + \omega\rho_3^{\pm}}{\sqrt{v^2+\omega^2}}, \quad H_5^{\pm} = \frac{v\eta_2^{\pm} + u\rho_1^{\pm}}{\sqrt{u^2+v^2}}. \quad (8)$$

For the odd W-particle spectrum, there exists a complex scalar particle

$$H'^0 = \frac{1}{\sqrt{u^2+w^2}}\left(u\chi_1^{0*} + w\eta_3^0\right). \quad (9)$$

For convenience, we list a few mass expressions for the physical fields that we will use for the calculations below

$$\begin{aligned} m_{H_1}^2 &= -\frac{fw}{\sqrt{2}}\left(\frac{v}{u} + \frac{u}{v}\right), \\ m_{\mathcal{A}}^2 &= -\frac{f}{\sqrt{2}}\left(\frac{uw}{v} + \frac{vw}{u} + \frac{uv}{w}\right), \\ m_{H_4}^2 &= \left(\frac{\lambda_7}{2} - \frac{fu}{\sqrt{2}vw}\right)\left(v^2+w^2\right), \\ m_{H_5}^2 &= \left(\frac{\lambda_8}{2} - \frac{fw}{\sqrt{2}uv}\right)\left(u^2+v^2\right). \end{aligned} \quad (10)$$

2.3 Fermion masses

The Yukawa interactions in the quark sector are written in [31] as follows

$$\begin{aligned} \mathcal{L}_{\text{Yukawa}}^{\text{quark}} &= h^U\bar{Q}_{3L}\chi U_R + h^D_{\alpha\beta}\bar{Q}_{\alpha L}\chi^* D_{\beta R} + h^u_a\bar{Q}_{3L}\eta u_{aR} \\ &\quad + h^d_a\bar{Q}_{3L}\rho d_{aR} + h^d_{\alpha a}\bar{Q}_{\alpha L}\eta^* d_{aR} \\ &\quad + h^u_{\alpha a}\bar{Q}_{\alpha L}\rho^* u_{aR} + H.c.. \end{aligned} \quad (11)$$

After symmetry breaking, the up-quarks and down-quarks receive mass. Their mixing mass matrices have the following form

$$\begin{aligned} m^u_{\alpha a} &= \frac{1}{\sqrt{2}}h^u_{\alpha a}v, \quad m^u_{3a} = -\frac{1}{\sqrt{2}}h^u_a u, \\ m^d_{\alpha a} &= -\frac{1}{\sqrt{2}}h^d_{\alpha a}u, \quad m^d_{3a} = -\frac{1}{\sqrt{2}}h^d_a v. \end{aligned} \quad (12)$$

In the general case, these matrices are not flavor-diagonal. They can be diagonalized by the unitary matrices $V_{u_{L,R}}$, $V_{d_{L,R}}$ as

$$\begin{aligned} V^\dagger_{u_L} m^u V_{u_R} &= \mathcal{M}_u = \text{Diag}(m_{u_1}, m_{u_2}, m_{u_3}), \\ V^\dagger_{d_L} m^d V_{d_R} &= \mathcal{M}_d = \text{Diag}(m_{d_1}, m_{d_2}, m_{d_3}). \end{aligned} \quad (13)$$

It means that the mass eigenstates relate to the flavor states by

$$\begin{aligned} u'_{L,R} &= (u'_{1L,R}, u'_{2L,R}, u'_{3L,R})^T \\ &= V^\dagger_{u_{L,R}}(u_{1L,R}, u_{2L,R}, u_{3L,R})^T, \\ d'_{L,R} &= (d'_{1L,R}, d'_{2L,R}, d'_{3L,R})^T \\ &= V^\dagger_{d_{L,R}}(d_{1L,R}, d_{2L,R}, d_{3L,R})^T. \end{aligned} \quad (14)$$

The CKM matrix is defined as $V_{\text{CKM}} = V^\dagger_{u_L}V_{d_L}$.

The Yukawa interactions for leptons are written by

$$\begin{aligned} \mathcal{L}_{\text{Yukawa}}^{\text{lepton}} &= h^e_{ab}\bar{\psi}_{aL}\rho e_{bR} \\ &\quad + h^\nu_{ab}\bar{\psi}_{aL}\eta\nu_{bR} + h'^\nu_{ab}\bar{\nu}^c_{aR}\nu_{bR}\phi + H.c.. \end{aligned} \quad (15)$$

The charged leptons have a Dirac mass $[M_l]_{ab} = -\frac{h^e_{ab}v}{\sqrt{2}}$. The flavor states e_a are related to the physical states e'_a by using two unitary matrices $U^l_{L,R}$ as

$$e_{aL} = (U^l_L)_{ab}e'_{bL}, \quad e_{aR} = (U^l_R)_{ab}e'_{bR}. \quad (16)$$

The neutrinos have both Dirac and Majorana mass terms. In the flavor states, $n_L = (\nu_L, \nu^c_R)^T$, the neutrino mass terms can be written as follows

$$\begin{aligned} \mathcal{L}^\nu_{\text{mass}} &= -\frac{1}{2}\bar{n}_L\begin{pmatrix} 0 & M^D_\nu \\ (M^D_\nu)^T & M^\nu_R \end{pmatrix}n_L + H.c. \\ &= -\frac{1}{2}\bar{n}_L M^\nu n_L + H.c., \end{aligned} \quad (17)$$

where $[M^D_\nu]_{ab} = -\frac{h^\nu_{ab}}{\sqrt{2}}u$, $[M^R_\nu]_{ab} = -\sqrt{2}h'^\nu_{ab}\Lambda$. The mass eigenstates n'_L are related to the neutrino flavor states as $n'_L =$

$U^{\nu\dagger} n_L$, where U^ν is a 6×6 matrix and written in terms of

$$U^\nu = \begin{pmatrix} U_L^\nu & V^\nu \\ (V^\nu)^T & U_R^\nu \end{pmatrix}. \tag{18}$$

The new neutral fermions N_a are a Majorana field, and they obtain their mass via effective interactions [32,33]. We suppose that the flavor states N_a relate to the mass eigenstates N'_a by using the unitary matrices $U^N_{L,R}$ as

$$N_{aL} = (U_L^N)_{ab} N'_{bL}, \quad N_{aR} = (U_R^N)_{ab} N'_{bR}. \tag{19}$$

2.4 Gauge bosons

Let us review the characteristics of the gauge sector. In addition to the SM gauge bosons, the 3-3-1-1 model also predicts six new gauge bosons: $X^{0,0*}$, $Y^\pm$, Z_2, Z_N. The gauge bosons are even W-parity except for the X, Y gauge bosons that carry odd W-parity. The masses of new gauge bosons have been given in [32,33] as

$$\begin{aligned} m^2_{Z_2} &\simeq \frac{g^2}{18}\Big\{(3+t_X^2)w^2 + 4t_N^2(w^2+9\Lambda^2) \\ &\quad - \sqrt{[(3+t_X^2)w^2 - 4t_N^2(w^2+9\Lambda^2)]^2 + 16(3+t_X^2)t_N^2 w^4}\Big\}, \end{aligned} \tag{20}$$

$$\begin{aligned} m^2_{Z_N} &\simeq \frac{g^2}{18}\Big\{(3+t_X^2)w^2 + 4t_N^2(w^2+9\Lambda^2) \\ &\quad + \sqrt{[(3+t_X^2)w^2 - 4t_N^2(w^2+9\Lambda^2)]^2 + 16(3+t_X^2)t_N^2 w^4}\Big\}, \\ m^2_W &= \frac{g^2}{4}(u^2+v^2), \quad m^2_X = \frac{g^2}{4}\left(u^2+w^2\right), \\ m^2_Y &= \frac{g^2}{4}\left(v^2+w^2\right). \end{aligned} \tag{21}$$

3 Rare processes mediated by new gauge bosons and new scalars at the tree-level

3.1 Meson mixing at tree level

In previous works [32,36], the authors have considered the FCNCs that couple to the new neutral gauge bosons Z_2 and Z_N at tree-level. Due to the different arrangements between generations of quarks, the SM quarks couple to two Higgs triplets. Therefore, there exist FCNCs coupled to the new neutral Higgs bosons at tree-level. These interactions derive from the Yukawa Lagrangian (11). After rotating to the physical basis via using Eqs. (12), (13), (14), we obtain the following

$$\begin{aligned} \mathcal{L}^{\text{Higgs}}_{\text{NC}} &= -\frac{g}{2m_W}\left(\bar{d}'_L \mathcal{M}_d d'_R + \bar{u}'_L \mathcal{M}_u u'_R\right) H \\ &\quad + \frac{g}{2m_W}\left(t_\beta \bar{d}'_L \mathcal{M}_d d'_R - \frac{1}{t_\beta}\bar{u}'_L \mathcal{M}_u u'_R\right) H_1 \\ &\quad + \frac{ig}{2m_W}\left(t_\beta \bar{d}'_L \mathcal{M}_d d'_R + \frac{1}{t_\beta}\bar{u}'_L \mathcal{M}_u u'_R\right)\mathcal{A} \\ &\quad + \frac{g}{2m_W}\left(\bar{d}'_L \Gamma^d d'_R + \bar{u}'_L \Gamma^u u'_R\right) H_1 \\ &\quad + \frac{ig}{2m_W}\left(\bar{d}'_L \Gamma^d d'_R - \bar{u}'_L \Gamma^u u'_R\right)\mathcal{A} + H.c., \end{aligned} \tag{22}$$

where $t_\beta = \tan\beta = \frac{v}{u}$, and Γ^u, Γ^d are defined as:

$$\begin{aligned} \Gamma^u_{ij} &= \frac{2}{s_{2\beta}}(V^\dagger_{u_L})_{i3}(V_{u_L})_{3k} m_{u_k} (V^\dagger_{u_R})_{ka}(V_{u_R})_{aj}, \\ \Gamma^d_{ij} &= -\frac{2}{s_{2\beta}}(V^\dagger_{d_L})_{i3}(V_{d_L})_{3k} m_{d_k} (V^\dagger_{d_R})_{ka}(V_{d_R})_{aj}. \end{aligned} \tag{23}$$

The first three terms of Eq. (22) are proportional to the quark mass matrices, and thus they are flavor-conserving interactions. The remaining terms are the FCNCs coupled to the new neutral Higgs bosons, including CP-even H_1 and CP-odd $\mathcal{A}$.

The Lagrangian of tree-level FCNCs mediated by Z_2, Z_N, which has been studied in [32], has the following form

$$\mathcal{L}^{\text{gauge}}_{\text{FCNC}} = -\sum_{q'=u',d'} \Theta^q_{ij}\left\{\bar{q}'_{iL}\gamma^\mu q'_{jL}(g_2 Z_{2\mu} + g_N Z_{N\mu})\right\}, \tag{24}$$

where

$$\begin{aligned} \Theta^q_{ij} &= \frac{1}{\sqrt{3}}(V^*_{q_L})_{3i}(V_{q_L})_{3j}, \\ g_2 &= g\left(\cos\xi\frac{1}{\sqrt{1-t_w^2/3}} + \sin\xi\frac{2t_N}{\sqrt{3}}\right), \\ g_N &= g\left(-\sin\xi\frac{1}{\sqrt{1-t_w^2/3}} + \cos\xi\frac{2t_N}{\sqrt{3}}\right). \end{aligned} \tag{25}$$

ξ is a mixing angle that is determined by $\tan 2\xi = \frac{4\sqrt{3+t_X^2}t_N w^2}{(3+t_X^2)w^2 - 4t_N^2(w^2+9\Lambda^2)}$, $t_N = \frac{g_N}{g}$, and $t_X = \frac{g_X}{g} = \frac{\sqrt{3}s_W}{\sqrt{3-4s_W^2}}$ with $s_W = \sin\theta_W$.

We now investigate the impact of FCNCs associated with both new gauge and scalar bosons on the oscillation of mesons. From FCNCs given in Eqs. (22)–(24), we obtain the effective Lagrangian that affects the meson mixing as

$$\begin{aligned} \mathcal{L}_{\text{effective}} &= \frac{g^2}{4m_W^2}\left\{(\Gamma^q_{ij})^2\left(\frac{1}{m^2_{H_1}} - \frac{1}{m^2_{\mathcal{A}}}\right)\left(\bar{q}'_{iL}q'_{jR}\right)^2\right. \\ &\quad \left.+(\Gamma^{q*}_{ji})^2\left(\frac{1}{m^2_{H_1}} - \frac{1}{m^2_{\mathcal{A}}}\right)\left(\bar{q}'_{iR}q'_{jL}\right)^2\right\} \\ &\quad + \frac{g^2}{4m_W^2}\left\{\Gamma^{q*}_{ji}\Gamma^q_{ij}\left(\frac{1}{m^2_{H_1}} + \frac{1}{m^2_{\mathcal{A}}}\right)\right. \\ &\quad (\bar{q}'_{iL}q'_{jR})(\bar{q}'_{iR}q'_{jL}) + \Gamma^{q*}_{ji}\Gamma^q_{ij} \\ &\quad \left.\left(\frac{1}{m^2_{H_1}} + \frac{1}{m^2_{\mathcal{A}}}\right)(\bar{q}'_{iR}q'_{jL})(\bar{q}'_{iL}q'_{jR})\right\} \end{aligned}$$

$$-\Theta_{ij}^2\left(\frac{g_2^2}{m_{Z_2}^2}+\frac{g_N^2}{m_{Z_N}^2}\right)(\bar{q}'_{iL}\gamma^\mu q'_{jL})^2, \tag{26}$$

with q denoting either u or d quark. This Lagrangian gives contributions to the mass difference of the meson systems as given

$$\begin{aligned}
(\Delta m_K)_{\rm NP} &= \Re\left\{\frac{2}{3}\Theta_{12}^2\left(\frac{g_2^2}{m_{Z_2}^2}+\frac{g_N^2}{m_{Z_N}^2}\right)\right.\\
&+\frac{5g^2}{48m_W^2}\left((\Gamma_{12}^d)^2+(\Gamma_{21}^{d*})^2\right)\left(\frac{1}{m_{H_1}^2}-\frac{1}{m_{\mathcal{A}}^2}\right)\\
&\left.\times\left(\frac{m_K}{m_s+m_d}\right)^2\right\}m_K f_K^2\\
&-\Re\left\{\frac{g^2\Gamma_{21}^{d*}\Gamma_{12}^d}{4m_W^2}\left(\frac{1}{m_{H_1}^2}+\frac{1}{m_{\mathcal{A}}^2}\right)\left(\frac{1}{6}+\frac{m_K^2}{(m_s+m_d)^2}\right)\right\}m_K f_K^2,\\
(\Delta m_{B_d})_{\rm NP} &= \Re\left\{\frac{2}{3}\Theta_{13}^2\left(\frac{g_2^2}{m_{Z_2}^2}+\frac{g_N^2}{m_{Z_N}^2}\right)\right.\\
&+\frac{5g^2}{48m_W^2}\left((\Gamma_{13}^d)^2+(\Gamma_{31}^{d*})^2\right)\\
&\left.\times\left(\frac{1}{m_{H_1}^2}-\frac{1}{m_{\mathcal{A}}^2}\right)\left(\frac{m_{B_d}}{m_b+m_d}\right)^2\right\}m_{B_d} f_{B_d}^2\\
&-\Re\left\{\frac{g^2\Gamma_{31}^{d*}\Gamma_{13}^d}{4m_W^2}\left(\frac{1}{m_{H_1}^2}+\frac{1}{m_{\mathcal{A}}^2}\right)\left(\frac{1}{6}+\frac{m_{B_d}^2}{(m_b+m_d)^2}\right)\right\}m_{B_d} f_{B_d}^2,\\
(\Delta m_{B_s})_{\rm NP} &= \Re\left\{\frac{2}{3}\Theta_{23}^2\left(\frac{g_2^2}{m_{Z_2}^2}+\frac{g_N^2}{m_{Z_N}^2}\right)\right.\\
&+\frac{5g^2}{48m_W^2}\left((\Gamma_{32}^{d*})^2+(\Gamma_{23}^d)^2\right)\\
&\left.\times\left(\frac{1}{m_{H_1}^2}-\frac{1}{m_{\mathcal{A}}^2}\right)\left(\frac{m_{B_s}}{m_s+m_b}\right)^2\right\}m_{B_s} f_{B_s}^2\\
&-\Re\left\{\frac{g^2\Gamma_{32}^{d*}\Gamma_{23}^d}{4m_W^2}\left(\frac{1}{m_{H_1}^2}+\frac{1}{m_{\mathcal{A}}^2}\right)\left(\frac{1}{6}+\frac{m_{B_s}^2}{(m_s+m_b)^2}\right)\right\}m_{B_s} f_{B_s}^2.
\end{aligned} \tag{27}$$

We would like to remind the reader that the theoretical predictions of the meson mass differences account for both SM and all tree-level contributions. It hints that meson mass differences can be separated as

$$\Delta m_{K,B_d,B_s} = (\Delta m_{K,B_d,B_s})_{\rm SM} + (\Delta m_{K,B_d,B_s})_{\rm NP}, \tag{28}$$

where the SM contributions to the meson mass differences are given by [37,38]

$$\begin{aligned}
(\Delta m_K)_{\rm SM} &= 0.467\times10^{-2}/ps,\\
(\Delta m_{B_d})_{\rm SM} &= (0.575^{+0.093}_{-0.090})/ps,\\
(\Delta m_{B_s})_{\rm SM} &= (18.6^{+2.4}_{-2.3})/ps.
\end{aligned} \tag{29}$$

The theoretical predictions, given in Eq. (28), are compared with the experimental values as given in [39,40]

$$\begin{aligned}
(\Delta m_K)_{\rm exp} &= 0.5293(9)\times10^{-2}/ps,\\
(\Delta m_{B_d})_{\rm exp} &= 0.5065(19)/ps,\\
(\Delta m_{B_s})_{\rm exp} &= 17.749(20)/ps.
\end{aligned} \tag{30}$$

However, due to the long-distance effect in Δm_K, the uncertainties in this system are considerable. Therefore, we require the theory to produce the data for the kaon mass difference within 30%, namely

$$-0.3 < \frac{(\Delta m_K)_{\rm NP}}{(\Delta m_K)_{\rm exp}} < 0.3. \tag{31}$$

The SM predictions for B-meson mass difference are more accurate than those of kaon, and we have the following constraints by combining quadrature of the relative errors in the SM predictions and measurements [41]

$$0.6 < \frac{(\Delta m_{B_d})_{\rm exp}}{(\Delta m_{B_d})_{\rm SM}} < 1.17, \quad 0.71 < \frac{(\Delta m_{B_s})_{\rm exp}}{(\Delta m_{B_s})_{\rm SM}} < 1.2, \tag{32}$$

or equivalently

$$-0.4 < \frac{(\Delta m_{B_d})_{\rm NP}}{(\Delta m_{B_d})_{\rm SM}} < 0.17, \quad -0.29 < \frac{(\Delta m_{B_s})_{\rm NP}}{(\Delta m_{B_s})_{\rm SM}} < 0.2. \tag{33}$$

Let us do a numerical study from a set of all the input parameters that are taken by [40,42–45]

$$\begin{aligned}
m_d &= 4.88(20), \quad m_s = 93.44(68),\\
m_b &= 4198(12), \quad m_t = 172.4(7)\times10^3,\\
f_K &= 155.7(3), \quad m_K = 497.611(13),\\
f_{B_d} &= 190(1.3), \quad m_{B_d} = 5279.65(12),\\
f_{B_s} &= 230(1.3), \quad m_{B_s} = 5366.88(14),\\
|(V_{\rm CKM})_{33}(V_{\rm CKM})_{31}^*| &= 0.0087(2),\\
|(V_{\rm CKM})_{33}(V_{\rm CKM})_{32}^*/(V_{\rm CKM})_{23}| &= 0.982(1),\\
|(V_{\rm CKM})_{23}| &= 0.04200(64).
\end{aligned} \tag{34}$$

All mass parameters are in MeV. Besides, we assume $t_N = 1$, $g = \sqrt{4\pi\alpha}/s_W$, where $\alpha = 1/128$ and $s_W^2 = 0.231$. The mixing matrix for right-handed quarks, V_{uR}, is a unitary matrix, whereas V_{dR} is parameterized by three mixing angles, θ_{12}^R, θ_{13}^R and θ_{23}^R, as

$$\mathrm{V}_{dR} = \begin{pmatrix} c_{12}^R c_{23}^R - s_{12}^R s_{13}^R s_{23}^R & -s_{12}^R c_{13}^R & -c_{12}^R s_{23}^R - s_{12}^R s_{13}^R c_{23}^R \\ s_{12}^R c_{23}^R + c_{12}^R s_{13}^R s_{23}^R & c_{12}^R c_{13}^R & -s_{12}^R s_{23}^R + c_{12}^R s_{13}^R c_{23}^R \\ c_{13}^R s_{23}^R & -s_{13}^R & c_{13}^R c_{23}^R \end{pmatrix}, \tag{35}$$

where $s_{ig}^R = \sin\theta_{ij}^R$, $c_{if}^R = \cos\theta_{ij}^R$. For instance, we can choose $\theta_{12}^R = \pi/6$, $\theta_{13}^R = \pi/4$ and $\theta_{23}^R = \pi/3$. The NP scales require the following constraints $w \sim \Lambda \sim -f \gg u, v$, due to the condition of diagonalization for the mixing mass matrices in [32].

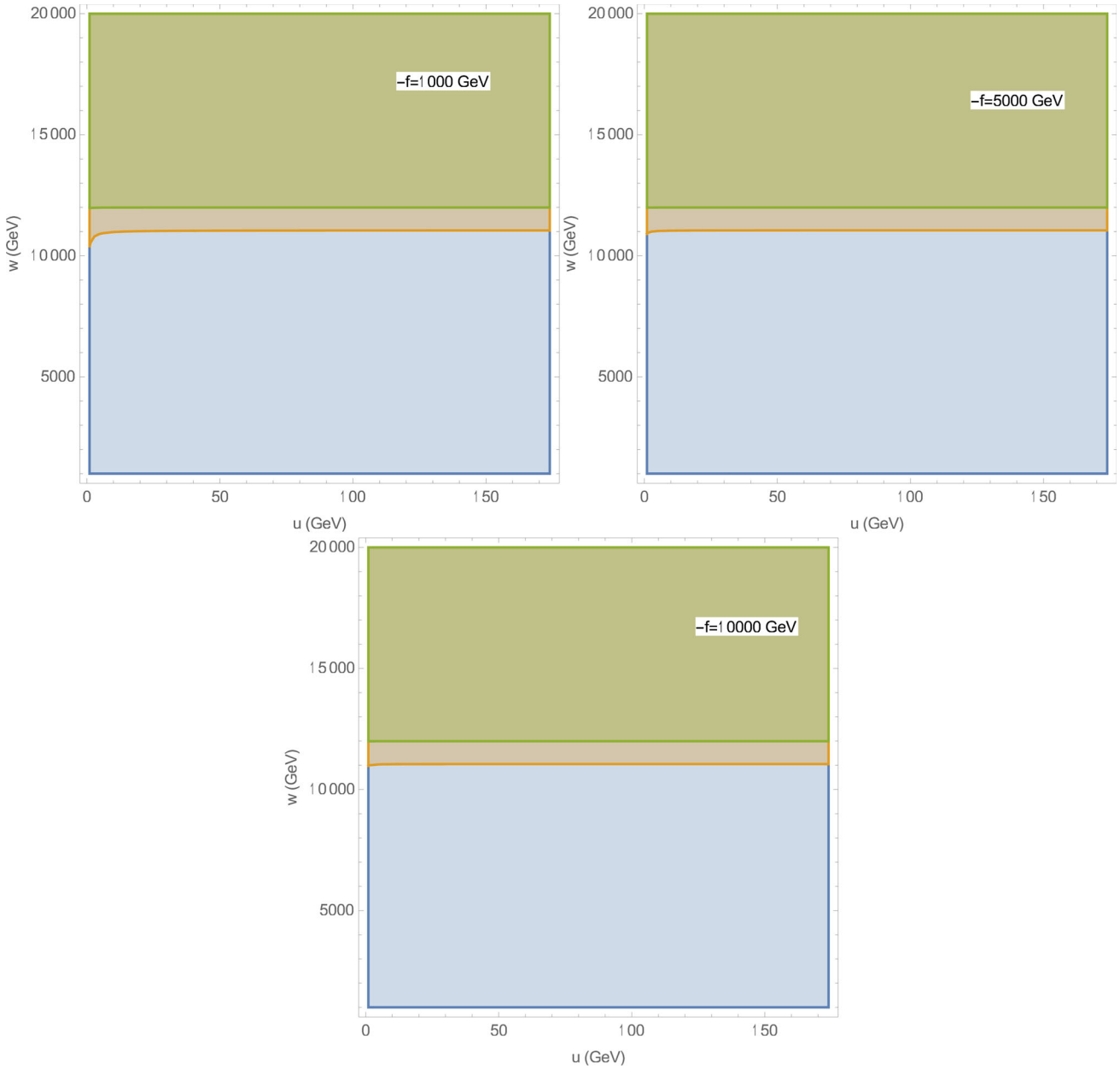

Fig. 1 Constraints for w and u from the meson mass differences Δm_K,Δm_{B_s} and Δm_{B_d}. The available region for Δm_K is the whole frame, whereas the orange and green regions are for Δm_{B_s} and Δm_{B_d}

We first study the role of FCNCs coupled to the scalar fields, H_1, $\mathcal{A}$, in meson mixing parameters. To see its effect, we change the f-parameter, which only affects the masses of the H_1, $\mathcal{A}$ (see in Eq. (10)). Specifically, in Fig. 1, we draw contours of the mass differences Δm_K, Δm_{B_s}, and Δm_{B_d}, as functions of the NP scale w and u for three different choices of f-parameter as $f = -1000$ GeV, $f = -5000$ GeV and $f = -10{,}000$ GeV. There are almost no differences between the three figures. That is, the mixing parameters are affected slightly by FCNCs coupled to the scalar fields.

Next, we consider the contributions of FCNCs coupled to new gauge bosons to the meson mixing parameters. To estimate how important they are, we compare their contributions with those of the new scalar bosons. The ratio of these two contributions is presented in Fig. 2. The results show that the significant contribution comes from the FCNCs of new gauge bosons. It once again clarifies the small effect of the new scalar fields on the meson mixing systems.

Finally, we investigate the constraints on the VEVs from $\Delta m_{K,B_s,B_d}$. In Fig. 1, the allowed region of parameters that satisfies the constraints given in Eqs. (31), (33) is the green

one. The electroweak symmetry breaking energy scale, u, is not constrained by conditions imposed on the meson mass mixing parameters. However, these conditions affect the NP scale w. From Fig. 1, we obtain a lower bound on the NP scale, $w > 12$ TeV. This lower bound is more stringent and is remarkably larger than that obtained previously [32]. This difference is because, in the previous study, the authors compared the NP contributions with experimental values and ignored the SM contributions to the theoretical predictions. Moreover, Eq. (131) in [32], the authors used $(\Delta m_{B_s})_{\rm NP} < \frac{1}{(100\ {\rm TeV})^2} m_{B_s} f_{B_s}^2 \simeq 41.2871/ps$, the upper limit for $(\Delta m_{B_s})_{\rm NP}$ is even greater than that of the experimental value given in Eq. (30). This is not reasonable because the theoretical prediction must consist of both SM and NP contributions. We must also consider the uncertainties of both SM and experimental predictions. Thus, the NP contributions have to be constrained by the conditions given in Eqs. (31, 33).

3.2 $B_s \to \mu^+\mu^-$, $B \to K^*\mu^+\mu^-$ and $B^+ \to K^+\mu^+\mu^-$

Rare decays of B meson, in particular of the decay induced by the quark level transition, $B_s \to \mu^+\mu^-$, $B \to K^*\mu^+\mu^-$ and $B^+ \to K^+\mu^+\mu^-$, are sensitive to physics beyond the SM. The NP effects can be quantified via the language of the effective theory. The effective Hamiltonian related to the above decays is determined by the quark FCNCs given in (22), (24) and the lepton flavor-conserving neutral currents (LFCNCs). The LFCNCs coupled to the neutral scalars, $H_1, \mathcal{A}$, obtained from Eq. (15) as follows

$$-\frac{g}{2m_W}\frac{u}{v}\bar{l}'_{aL}M^{lD}_{ab}l'_{bR}(H_1 + i\mathcal{A}) + H.c., \tag{36}$$

where $M^{lD} = {\rm Diag}(m_e, m_\mu, m_\tau)$. It is worth noting that there is no neutral Higgs mediated FCNC in the lepton sector. The interactions of Z_2 and Z_N with two charged leptons have been written in [31] read

$$\begin{aligned}&-\frac{g}{2c_W}\bar{f}\gamma^\mu\left(g_V^{Z_2}(f) - g_A^{Z_2}(f)\gamma_5\right) f Z_{2\mu}\\ &-\frac{g}{2c_W}\bar{f}\gamma^\mu\left(g_V^{Z_N}(f) - g_A^{Z_N}(f)\gamma_5\right) f Z_{N\mu},\end{aligned} \tag{37}$$

where the form of coefficients $g_V^{Z_2,Z_N}$, $g_A^{Z_2,Z_N}$ are found in [31].

Combining the quark FCNCs and the LFCNCs, we obtain the effective Hamiltonian for $B_s \to \mu^+\mu^-$, $B \to K^*\mu^+\mu^-$ and $B^+ \to K^+\mu^+\mu^-$ processes as follows

$$\begin{aligned}\mathcal{H}_{\rm eff} = -\frac{4G_F}{\sqrt{2}}V_{tb}V_{ts}^* \sum_{i=9,10,S,P}&(C_i(\mu)\mathcal{O}_i(\mu)\\ &+ C'_i(\mu)\mathcal{O}'_i(\mu)),\end{aligned} \tag{38}$$

where the operators are defined by

$$\begin{aligned}\mathcal{O}_9 &= \frac{e^2}{(4\pi)^2}(\bar{s}\gamma_\mu P_L b)(\bar{l}\gamma^\mu l),\\ \mathcal{O}_{10} &= \frac{e^2}{(4\pi)^2}(\bar{s}\gamma_\mu P_L b)(\bar{l}\gamma^\mu\gamma^5 l),\\ \mathcal{O}_S &= \frac{e^2}{(4\pi)^2}(\bar{s}P_R b)(\bar{l}l),\end{aligned} \tag{39}$$

$$\mathcal{O}_P = \frac{e^2}{(4\pi)^2}(\bar{s}P_R b)\left(\bar{l}\gamma_5 l\right). \tag{40}$$

The operators $\mathcal{O}'_{9,10,S,P}$ are obtained from $\mathcal{O}_{9,10,S,P}$ by replacing $P_L \leftrightarrow P_R$. Their Wilson coefficients consist of the SM leading and tree-level NP contributions. For $C_{9,10}$ we split into the SM and NP contributions as: $C_{9,10} = C^{\rm SM}_{9,10} + C^{\rm NP}_{9,10}$, where the central points of $C^{\rm SM}_{9,10}$ are given in [46], $C^{\rm SM}_{10} = -4.198$, $C^{\rm SM}_9 = 4.344$, and the $C^{\rm NP}_{9,10,S,P}$ are written by

$$\begin{aligned}C^{\rm NP}_9 &= -\Theta_{23}\frac{m_W^2}{c_W V_{tb}V_{ts}^*}\frac{(4\pi)^2}{e^2}\left(\frac{g_2}{g}\frac{g_V^{Z_2}(f)}{m^2_{Z_2}} + \frac{g_N}{g}\frac{g_V^{Z_N}(f)}{m^2_{Z_N}}\right),\\ C^{\rm NP}_{10} &= \Theta_{23}\frac{m_W^2}{c_W V_{tb}V_{ts}^*}\frac{(4\pi)^2}{e^2}\left(\frac{g_2}{g}\frac{g_A^{Z_2}(f)}{m^2_{Z_2}} + \frac{g_N}{g}\frac{g_A^{Z_N}(f)}{m^2_{Z_N}}\right).\end{aligned} \tag{41}$$

Noting that $C^{\rm SM}_{S,P} = C'^{\rm SM}_{S,P} = 0$. Therefore, the $C_{S,P}$, $C'_{S,P}$ are obtained by NP contributions as follows

$$\begin{aligned}C^{\rm NP}_S &= \frac{8\pi^2}{e^2}\frac{1}{V_{tb}V_{ts}^*}\frac{\Gamma^d_{23}\Gamma^l_{\alpha\alpha}}{m^2_{H_1}},\\ C'^{\rm NP}_S &= \frac{8\pi^2}{e^2}\frac{1}{V_{tb}V_{ts}^*}\frac{\left(\Gamma^d_{32}\right)^*\Gamma^l_{\alpha\alpha}}{m^2_{H_1}},\\ C^{\rm NP}_P &= -\frac{8\pi^2}{e^2}\frac{1}{V_{tb}V_{ts}^*}\frac{\Gamma^d_{23}\Delta^l_{\alpha\alpha}}{m^2_{A}},\\ C'^{\rm NP}_P &= \frac{8\pi^2}{e^2}\frac{1}{V_{tb}V_{ts}^*}\frac{\left(\Gamma^d_{32}\right)^*\Delta^l_{\alpha\alpha}}{m^2_{A}},\end{aligned} \tag{42}$$

where $\Gamma^l_{\alpha\alpha} = \Delta^l_{\alpha a} = \frac{u}{v}m_{l_\alpha}$.

From the effective Hamiltonian given in (38), we obtain the branching ratio of the $B_s \to l^+_\alpha l^-_\alpha$ decay

$$\begin{aligned}{\rm Br}(B_s \to l^+_\alpha l^-_\alpha)_{\rm theory} &= \frac{\tau_{B_s}}{64\pi^3}\alpha^2 G_F^2 f_{B_s}^2\\ &\times|V_{tb}V_{ts}^*|^2 m_{B_s}\sqrt{1-\frac{4m^2_{l_\alpha}}{m^2_{B_s}}}\\ &\times\left\{\left(1-\frac{4m^2_{l_\alpha}}{m^2_{B_s}}\right)\left|\frac{m^2_{B_s}}{m_b+m_s}\left(C_S - C'_S\right)\right|^2\right.\\ &\left.+\left|2m_{l_\alpha}\left(C_{10}-C'_{10}\right) + \frac{m^2_{B_s}}{m_b+m_s}\left(C_P - C'_P\right)\right|^2\right\},\end{aligned} \tag{43}$$

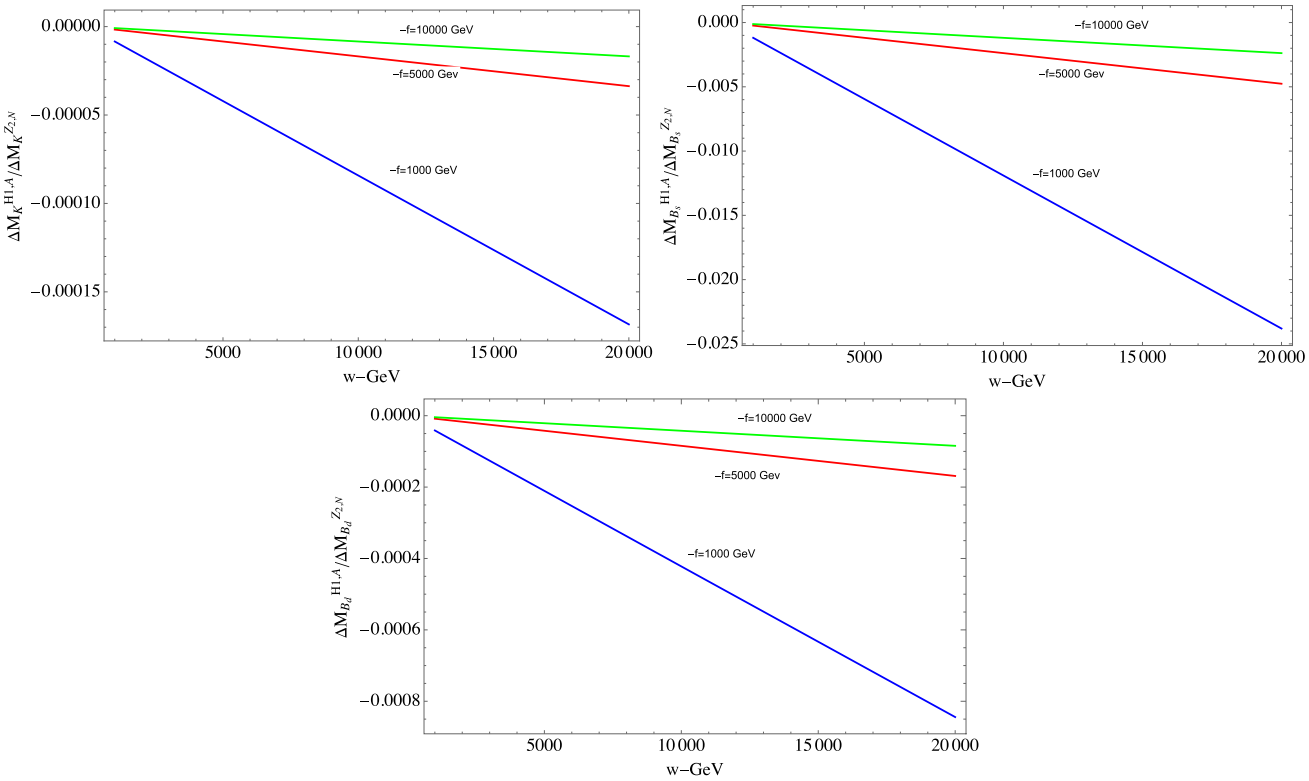

Fig. 2 The figures present the dependence of ratios $\Delta m^{H_1,A}_{K,B_s,B_d}/\Delta m^{Z_2,Z_N}_{K,B_s,B_d}$ on the NP scale w

where τ_{B_s} is the total lifetime of the B_s meson. If including the effect of oscillations in the $B_s - \bar{B}_s$ system, the theoretical and experimental results are related by [47]

$$\mathrm{Br}(B_s \to l_\alpha^+ l_\alpha^-)_{\mathrm{exp}} \simeq \frac{1}{1-y_s}\mathrm{Br}(B_s \to l_\alpha^+ l_\alpha^-)_{\mathrm{theory}}, \tag{44}$$

where $y_s = \frac{\Delta\Gamma_{B_s}}{2\Gamma_{B_s}} = 0.0645(3)$ [39]. For $B_s \to e^+e^-$, the SM prediction [48] is

$$\mathrm{Br}(B_s \to e^+e^-)_{\mathrm{SM}} = (8.54 \pm 0.55) \times 10^{-14}, \tag{45}$$

and the experimental bound has been given in [49] as

$$\mathrm{Br}(B_s \to e^+e^-)_{\mathrm{exp}} < 2.8 \times 10^{-7}. \tag{46}$$

The SM contribution to the branching ratio of $B_s \to e^+e^-$ is strongly suppressed to the current experimental upper bound. It may be an excellent place to look for NP. Completely contrary to $B_s \to e^+e^-$, the very recent measurement of the branching ratio $(B_s \to \mu^+\mu^-)$ is given by [7]

$$\mathrm{Br}(B_s \to \mu^+\mu^-)_{\mathrm{exp}} = (3.09^{+0.46\ +0.15}_{-0.43\ -0.11}) \times 10^{-9}. \tag{47}$$

This experimental upper bound closes to the central value of the SM prediction (including the effect of $B_s - \bar{B}_s$ oscillations) that has been studied in [50]

$$\mathrm{Br}\left(B_s \to \mu^+\mu^-\right)_{\mathrm{SM}} = (3.66 \pm 0.14) \times 10^{-9}. \tag{48}$$

It shows that experimental results are in slight tension with the SM prediction of $\mathrm{Br}(B_s \to \mu^+\mu^-)$. NP effects in $B_s \to \mu^+\mu^-$ lead to new stringent constraints on NP scale. Let us concentrate on the numerical study of $B_s \to \mu^+\mu^-$.

In Fig. 3, the red curve in the left panel demonstrates the $\mathrm{Br}(B_s \to \mu^+\mu^-)$ in the 3-3-1-1 model as a function of the new symmetry breaking scale. The predicted results are only consistent with the current experimental bounds if the VEV, w, is larger than 5 TeV. This bound is not as strict as the constraints obtained from studying the meson oscillations in Sect. 3.1. So, the best fit region pulls for both $(\bar{B}_s - B_s)$ mixing and $\mathrm{Br}(B_s \to \mu^+\mu^-)$ experimental bounds is $w > 12$ TeV. In the right panel of Fig. 3, we draw the NP contributions to each Wilson coefficient. Compared to the $C^{\mathrm{NP}}_{9,10}$, the $C_{\mathrm{S,P}}$ are further suppressed by a factor of $10^{-4} \div 10^{-5}$. So, the main contribution of the NP to the $\mathrm{Br}(B_s \to \mu^+\mu^-)$ comes from the C^{NP}_{10}. In the limit $w > 12$ TeV, the C^{NP}_{10} is positive. It causes the $\mathrm{Br}(B_s \to \mu^+\mu^-)$ reduced about 5% , which brings the theoretical prediction and experimental values get closer together.

If the C^{NP}_{10} affects the decay process $B_s \to \mu^+\mu^-$, the C^{NP}_9 plays a crucial role in $B \to K^*\mu^+\mu^-$ decay. The current experimental measurements of the $b \to s\mu^+\mu^-$ have attracted and led to many model-independent global analyses [51–58] assuming the presence of NP. The anomalies of the $B \to K^*\mu^+\mu^-$ decay were explained if there exists a large

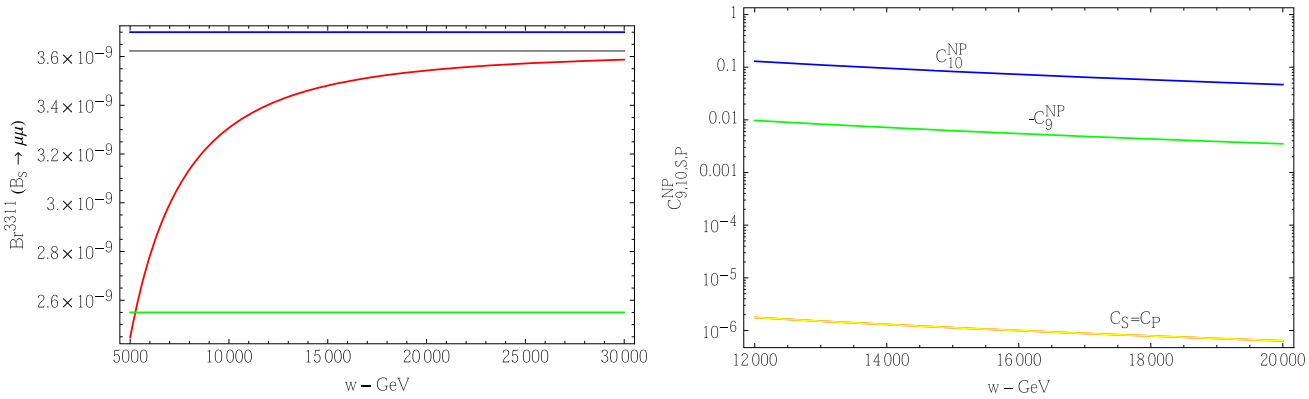

Fig. 3 The left panel draws the Br($B_s \to \mu^+\mu^-$): red curve presents the prediction values of the 3-3-1-1 model, gray line represents the central values of the SM prediction. The blue and green lines represent the experimental upper and lower bounds. The right panel predicts the NP contributions to the Wilson coefficients. Here both panels are plotted by fixing: $\Lambda = 1000w$, $f = -w$, $u = 200$ GeV. Other parameters are selected as done in the Sect. 3

negative contribution to the Wilson coefficient $C_9^{\rm NP}$. The best-fit point for the $C_9^{\rm NP}$ varies around -1.1. The green line in the right panel of Fig. 3 predicts the $C_9^{\rm NP}$ in the 3-3-1-1 model. In the limit, $w > 12$ TeV, we obtain its maximal prediction value $C_9^{\rm NP} \simeq -0.01$. So, the NP coming from the 3-3-1-1 model can not explain the anomalies of $B \to K^*\mu^+\mu^-$ process.

The measurements of the branching fraction of the decay $B^+ \to K^+\mu^+\mu^-$ [23,24] have turned out to be slightly on the low side compared to SM expectations. Both the C_9, C_{10} contribute to the Br $\left(B^+ \to K^+\mu^+\mu^-\right)$. As predicted by the 3-3-1-1 model, the NP contribution to these parameters is minimal (see Fig. 3) because the NP scale satisfies the constraint $w > 12$ TeV. Both the $C_9^{\rm NP}$ and $C_{10}^{\rm NP}$ are too low and far from the values of global analysis, see in [51–54]. Thus, we believe that the NP effects in $B^+ \to K^+\mu^+\mu^-$ remain small in the 3-3-1-1 model.

4 Radiative processes

4.1 $b \to s\gamma$ decay

The branching fraction and the photon energy spectrum of the radiative penguin $b \to s\gamma$ process have been firstly reported by CLEO experiment, Br($b \to s\gamma$) $= (3.21 \pm 0.43 \pm 0.27^{+0.18}_{-0.10}) \times 10^{-4}$ [8]. Recently, HFLAV group has obtained the average result by combining the measurements from CLEO, BaBar and Belle, Br($b \to s\gamma$) $= (3.32 \pm 0.15) \times 10^{-4}$ [39] for a photon-energy cut-off $E_\gamma > 1.6$ GeV. This result is in good agreement with the SM prediction up to Next-to-Next-to-Leading Order (NNLO) Br($b \to s\gamma$) $= (3.36 \pm 0.23) \times 10^{-4}$ [59,60], with the same energy cut-off E_γ. It suggests that the NP contributions to this process, if any, have to be small. Thus, studying the $b \to s\gamma$ decay can give a strong constraint on the NP scale. The radiative process $b \to s\gamma$ is most conveniently described in the framework of an effective theory that arises after decoupling of new particles. Excluding the charged currents associated with the $W_\mu^\pm$ gauge boson, the 3-3-1-1 model contains new charged currents, which couple to the new charged gauge bosons $Y_\mu^\pm$, two charged Higgs bosons $H_4^\pm$, $H_5^\pm$, and the FCNCs coupled to the $Z_{2,N}$ as given in Eq. (24). All of the above currents generate the $b \to s\gamma$ process.

Let us write down the charged scalar currents related to $b \to s\gamma$. The $H_4^\pm$ only couples to the exotic quarks, so it does not create the flavor-changing charged currents (FCCCs) for SM quarks. While $H_5^\pm$ couples to the SM quarks and creates the scalar FCCCs. The relevant Lagrangian is

$$\mathcal{L}_{\rm Yukawa}^{H_5^\pm} = \frac{g}{\sqrt{2}m_W}\left\{\bar{d}'_L\mathcal{X}\mathcal{M}_u u'_R + \bar{d}'_R\mathcal{M}_d\mathcal{Y}u'_L\right\}H_5^- + H.c., \tag{49}$$

where $\mathcal{Y} = t_\beta V_{\rm CKM}^\dagger - \frac{2}{s_{2\beta}}\mathcal{T}$ and $\mathcal{X} = \frac{1}{t_\beta}V_{\rm CKM}^\dagger - \frac{2}{s_{2\beta}}\mathcal{T}$. The $\mathcal{T}$ is defined as $\mathcal{T}_{ij} = (V_{d_L}^\dagger)_{i3}(V_{u_L})_{3j}$, $s_{2\beta} = \sin 2\beta$, $t_{2\beta} = \tan 2\beta$. The charged currents associated with the $W^\pm$, $Y^\pm$, are described by the V-A currents as follows

$$\begin{aligned}\mathcal{L}_{W,Y}^{\rm quark} &= \frac{g}{2\sqrt{2}}\bar{u}'\gamma^\mu(1-\gamma_5)W_\mu^+ V_{\rm CKM}d' + H.c.\\ &+\frac{g}{2\sqrt{2}}\left\{\bar{d}'_j(V_{d_L}^*)_{j3}\gamma^\mu(1-\gamma_5)Y_\mu^- U\right.\\ &\left.+\bar{D}_\alpha\gamma^\mu(1-\gamma_5)Y_\mu^-(V_{u_L})_{\alpha j}u'_j\right\} + H.c..\end{aligned} \tag{50}$$

The effective Hamiltonian for the decay $b \to s\gamma$ is

$$\begin{aligned}\mathcal{H}_{\rm eff}^{b\to s\gamma} &= -\frac{4G_F}{\sqrt{2}}V_{tb}V_{ts}^*[C_7(\mu_b)\mathcal{O}_7\\ &+C_8(\mu_b)\mathcal{O}_8 + C'_7(\mu_b)\mathcal{O}'_7 + C'_8(\mu_b)\mathcal{O}'_8],\end{aligned} \tag{51}$$

with $\mu_b = \mathcal{O}(m_b)$. The electromagnetic and chromomagnetic dipole operators $\mathcal{O}_7, \mathcal{O}_8$ are defined as

$$\mathcal{O}_7 = \frac{e}{(4\pi)^2} m_b (\bar{s}_\alpha \sigma_{\mu\nu} P_R b_\alpha) F^{\mu\nu},$$
$$\mathcal{O}_8 = \frac{g_s}{(4\pi)^2} m_b (\bar{s}_\alpha \sigma_{\mu\nu} T^a_{\alpha\beta} P_R b_\beta) G^{a\mu\nu}, \quad (52)$$

and the primed operators $\mathcal{O}'_{7,8}$ are obtained by replacing $P_L \leftrightarrow P_R$. The Wilson coefficients $C_{7,8}(\mu_b)$ split as the sum of the SM and 3-3-1-1 contributions

$$C_{7,8}(\mu_b) = C^{\rm SM}_{7,8}(\mu_b) + C^{\rm NP}_{7,8}(\mu_b). \quad (53)$$

Note that the Wilson coefficients $C'_{7,8}$ will be ignored in our calculation since they are suppressed by the ratio m_s/m_b. The SM Wilson coefficients $C^{\rm SM}_{7,8}$ at the scale $\mu \sim m_W$ are first given by [61]

$$C_7^{\rm SM(0)}(m_W) = \frac{m_t^2}{m_W^2} f_\gamma\left(\frac{m_t^2}{m_W^2}\right),$$
$$C_8^{\rm SM(0)}(m_W) = \frac{m_t^2}{m_W^2} f_g\left(\frac{m_t^2}{m_W^2}\right), \quad (54)$$

where the index 0 indicates that the Wilson coefficients are calculated without QCD correction.

The NP contributes to $C^{\rm NP}_{7,8}$ at the quantum level via the higher order charged current interactions in Eqs. (49), (50) and the FCNCs given in Eq. (24). They can be split into each contribution as follows

$$C^{\rm NP(0)}_{7,8} = C^{H_5(0)}_{7,8}(m_{H_5}) + C^{Y(0)}_{7,8}(m_Y) + C^{Z_{2,N}(0)}_{7,8}(m_{Z_{2,N}}), \quad (55)$$

where

$$C_7^{H_5(0)}(m_{H_5}) = \frac{m_t^2}{m_{H_5}^2}\left[\frac{1}{3}t_\beta^2 f_\gamma\left(\frac{m_t^2}{m_{H_5}^2}\right) + f'_\gamma\left(\frac{m_t^2}{m_{H_5}^2}\right)\right],$$
$$C_8^{H_5(0)}(m_{H_5}) = \frac{m_t^2}{m_{H_5}^2}\left[\frac{1}{3}t_\beta^2 f_g\left(\frac{m_t^2}{m_{H_5}^2}\right) + f'_g\left(\frac{m_t^2}{m_{H_5}^2}\right)\right],$$
$$C_7^{Y(0)}(m_Y) = \frac{m_W^2}{m_Y^2}\frac{m_U^2}{m_Y^2} f_\gamma\left(\frac{m_U^2}{m_Y^2}\right),$$
$$C_8^{Y(0)}(m_Y) = \frac{m_W^2}{m_Y^2}\frac{m_U^2}{m_Y^2} f_g\left(\frac{m_U^2}{m_Y^2}\right), \quad (56)$$

with all functions $f_{\gamma,g}$ and $f'_{\gamma,g}$ are defined as shown below

$$f_\gamma(x) = \frac{(7-5x-8x^2)}{24(x-1)^3} + \frac{x(3x-2)}{4(x-1)^4}\ln x,$$
$$f'_\gamma(x) = \frac{(3-5x)}{12(x-1)^2} + \frac{(3x-2)}{6(x-1)^3}\ln x,$$
$$f_g(x) = \frac{2+5x-x^2}{8(x-1)^3} - \frac{3x}{4(x-1)^4}\ln x,$$
$$f'_g(x) = \frac{3-x}{4(x-1)^2} - \frac{1}{2(x-1)^3}\ln x. \quad (57)$$

The $C_7^{Z_{2,N}(0)}(m_{Z_{2,N}})$ are obtained by the FCNCs coupled to the $Z_{2,N}$ and have a form as given in [63]

$$C_7^{Z_{2,N}(0)}(m_{Z_{2,N}}) = -\frac{2}{9g^2}\frac{m_W^2}{m_{Z_{2,N}}^2}\sum_{f=d,s,b}\frac{g_L^{fs*}g_L^{fb}}{V_{ts}^*V_{tb}} + \frac{2}{3g^2}\frac{m_W^2}{m_{Z_{2,N}}^2}\sum_{f=d,s,b}\frac{m_f}{m_b}\frac{g_L^{fs*}g_R^{fb}}{V_{ts}^*V_{tb}},$$
$$C_8^{Z_{2,N}(0)}(m_{Z_{2,N}}) = -3C_7^{Z_{2,N}}(m_{Z_{2,N}}) \quad (58)$$

with $g^{ff}_{L,R} = [g_V^{Z_{2,N}}(f) \pm g_A^{Z_{2,N}}(f)]/2$ are the flavor-conversing couplings given in [31] while $g^{fs,fb}$ are the flavor-violating couplings defined in Eq. (24).

Noting that QCD corrections to $b \to s\gamma$ are important and have to be included to complete the analysis. The Ref. [62] predicted $C^{\rm SM}_{7,8}$ up to NNLO, $C_7^{\rm SM}(\mu_b) = -0.3523$ for $\mu_b = 2.5$ GeV. The recent calculations of the NP contributions to the $C^{\rm NP}_{7,8}$ have been considered at the Leading Order (LO) [63,64]. In the following work, we study the effect of QCD corrections on the $C^{\rm NP}_{7,8}$ at the LO. In the 3-3-1-1 model, there are four heavy scales: m_Y, $m_{Z_{2,N}}$ and m_{H_5} . The difference between these scales can be ignored because the effects of QCD running are less important at high energies. Hence, we assume all calculations are at the same scale. For instance, we choose $\mu \sim m_Y$. The QCD corrections for $C_7^{Z_{2,N}}$ are given by

$$C_7^{Z_{2,N}}(\mu_b) = \kappa_7 C_7^{Z_{2,N}}(m_Y) + \kappa_8 C_8^{Z_{2,N}}(m_Y) + \Delta_{Z_{Z_{2,N}}}(\mu_b), \quad (59)$$

where $\kappa_{7,8}$ are NP magic numbers $\kappa_7 = 0.39$, $\kappa_8 = 0.130$ at $\mu \sim 10$ TeV [64]. $\Delta_{Z_{2,N}}(\mu_b)$ are the contributions coming from the mixing of new neutral current-current operators, generated by the exchange of $Z_{2,N}$ with the dipole operators $\mathcal{O}_{7,8}$

$$\Delta_{Z_{Z_{2,N}}}(\mu_b) = \sum_{\substack{A=L,R,\\ f=u,c,t,d,s,b}} \kappa^f_{LA}\Delta_{LA}C_2^f(w) + \sum_{A=L,R}\hat{\kappa}^d_{LA}\Delta_{LA}\hat{C}_2^d(w),$$
$$\Delta_{LA}C_2^f(m_Y) = -\frac{2}{g^2}\frac{g_L^{sb*}g_A^{ff}}{V_{ts}^*V_{tb}},$$
$$\Delta_{LA}\hat{C}_2^d(m_Y) = -\frac{2}{g^2}\frac{g_L^{sd*}g_A^{bd}}{V_{ts}^*V_{tb}} \quad (60)$$

For $w = 10$ TeV, we have $m_Y \simeq 3.2$ TeV, and obtain $C_7^{Z_{2,N}}(\mu_b) \simeq \mathcal{O}(10^{-5})$, which is strongly suppressed by the SM prediction, $C_7^{\rm SM}(\mu_b) = -0.3523$. Therefore, in the next calculation, $C_7^{Z_{2,N}}$ can be ignored. If including the LO of QCD corrections, the C_7^Y and $C_7^{H_5}$ have the form as [63,64]

$$C_7^Y(\mu_b) = \kappa_7 C_7^Y(m_Y) + \kappa_8 C_8^Y(m_Y),$$

$$C_7^{H_5}(\mu_b) = \kappa_7 C_7^{H_5}(m_Y) + \kappa_8 C_8^{H_5}(m_Y). \quad (61)$$

The branching ratio $\mathrm{Br}(b \to s\gamma)$ is given as

$$\mathrm{Br}(b \to s\gamma) = \frac{6\alpha}{\pi C}\frac{|V_{ts}^* V_{tb}|^2}{|V_{cb}|^2}(|C_7(\mu_b)|^2 + N(E_\gamma))\mathrm{Br}(b \to ce\bar{\nu}_e), \quad (62)$$

where $N(E_\gamma) = 3.6(6) \times 10^{-3}$ is a non-perturbative contribution, $C = |V_{ub}/V_{cb}|^2\Gamma(b \to ce\bar{\nu}_e)/\Gamma(b \to ue\bar{\nu}_e) = 0.580(16)$ [62] and branching ratio for semi-leptonic decay $\mathrm{Br}(b \to ce\bar{\nu}_e) = 0.1086(35)$ [40]. Other parameters are input as in Sect. 3.1.

The $\mathrm{Br}(b \to s\gamma)$ behaves as a function of the new particle masses, such as m_Y, m_{H_5}, m_U. These masses are understood as free parameters. In the limit, $u, v \ll -f\frac{u^2+v^2}{uv} \sim w \sim \Lambda$, they can be rewritten as

$$m_Y^2 \simeq \frac{g^2 w^2}{4}, \quad m_{H_5}^2 \simeq \frac{w^2}{\sqrt{2}}, \quad m_U = -\frac{h^U w}{\sqrt{2}}, \quad (63)$$

where, $g = \sqrt{4\pi\alpha/s_W^2} \simeq 0.63$, h^U is unknown parameter. So, m_U is arbitrary at the TeV energy scale, which can be higher or smaller than two other masses, m_{H_5}, m_Y. Without loss of generality, we investigate the mass hierarchy of new particles according to three scenarios: $m_{H_5} > m_Y > m_U$, $m_{H_5} > m_U > m_Y$, and $m_U > m_{H_5} > m_Y$.

In Fig. 4, we show the dependence of $\mathrm{Br}(b \to s\gamma)$ on the NP scale w in the limit $u, v \ll -f\frac{u^2+v^2}{uv} \sim w \sim \Lambda$. Each panel corresponds to the scenarios of mass hierarchy and three different choices of t_β. We see that the branching ratio strongly depends on the values of t_β where the term containing t_β comes from $C_7^{H_5}$. So we conclude that $C_7^{H_5}$ plays an important role in the radiative decay process $b \to s\gamma$. This is true for all three scenarios of the mass hierarchy. Besides, Fig. 4 indicates that the mass hierarchy does not affect $\mathrm{Br}(b \to s\gamma)$ much. This result is understood as the main contribution coming from $C_7^{H_5}$, and it is stronger than other contributions by the coefficient t_β^2. In the large t_β limit, the $\mathrm{Br}(b \to s\gamma) \simeq |C_7^{H_5}|^2 \simeq \frac{t_\beta^2}{w^2}$. The lower bound on the NP scale depends on the value of the t_β, specifically, $w \geq 1$ TeV for $t_\beta = 1$; $w \geq 4.1$ TeV for $t_\beta = 10$; $w \geq 7.7$ TeV for $t_\beta = 20$. These limits are weaker than the ones mentioned above.

To close this section, we consider the influence of NP on the $\mathrm{Br}(b \to s\gamma)$ in the limit $u, v \ll -f \sim w \sim \Lambda$. In Fig. 5, we see that the dependence of branching ratio on t_β is not as strong as predicted in Fig. 4. This difference can be explained by the dependence of m_{H_5} on t_β, $m_{H_5} = 0.85w\sqrt{(t_\beta + 1/t_\beta)}$. Therefore, $\mathrm{Br}(b \to s\gamma) \simeq |C_7^{H_5}|^2 \simeq t_\beta^2\frac{1}{m_{H_5}^2} \simeq t_\beta\frac{1}{w^2}$, whereas $\mathrm{Br}(b \to s\gamma) \simeq t_\beta^2\frac{1}{w^2}$ for the previous case. This leads to the lower limit of the NP also changing for each choice of t_β. In the limit given in Sect. 3.1, $w > 12$ TeV, the affect of t_β to $\mathrm{Br}(b \to s\gamma)$ becomes trivial and the predicted branching ratio approaches the central value of the experimental bounds.

4.2 Charged lepton flavor violation

The charged lepton flavor violation (CLFV) processes are strongly suppressed in the SM with right-handed neutrinos, $\mathrm{Br}(l_i \to l_j\gamma) \simeq 10^{-55}$. Meanwhile, the current experimental bounds limits are given as [40]

$$\begin{aligned}&\mathrm{Br}(\mu^- \to e^-\gamma) < 4.2 \times 10^{-13},\\ &\mathrm{Br}(\tau^- \to e^-\gamma) < 3.3 \times 10^{-8},\\ &\mathrm{Br}(\tau^- \to \mu^-\gamma) < 4.4 \times 10^{-8}.\end{aligned} \quad (64)$$

It implies that the CLFV processes open a large window for studying the NP signals beyond the SM. Note that in the SM with right-handed neutrinos, the decay processes, $l_i \to l_j\gamma$, come from the one-loop level with $W^\pm$ mediated in the loop. The $\mathrm{Br}(l_i \to l_j\gamma)$ is suppressed due to the mixing matrix elements of the neutrinos. The 3-3-1-1 model anticipates the existence of additional charged currents associated with the new charged particles, $Y^\pm$, $H_{4,5}^\pm$. Consequently, the new one-loop diagrams in the model may contribute significantly to the $\mathrm{Br}\left(l_i \to l_j\gamma\right)$. This branching ratio may reach the upper experimental bound given in Eq. (64). In order to study the CLFV processes, we first write down the relevant Lagrangian based on the physical states as follows

$$\begin{aligned}\mathcal{L}_{\mathrm{Scalar}}^{\mathrm{lepton}} \supset\ & \frac{h_{ab}^e u}{\sqrt{u^2+v^2}}\left(\bar{\nu}'_{kL}(U_L^{\nu*})_{ka} + \overline{(\nu'_{kR})^c}V_{ka}^{\nu*}\right)\\ &\times(U_R^l)_{bj}e'_{jR}H_5^+ + \frac{h_{ab}^e\omega}{\sqrt{v^2+\omega^2}}\overline{(N'_{kR})^c}(U_R^N)_{ka}\\ &\times(U_R^l)_{bj}e'_{jR}H_4^+\\ &+\frac{h_{ab}^\nu v}{\sqrt{u^2+v^2}}\bar{e}'_{jL}(U_L^{l*})_{ja}\left((V^{\nu T})_{bk}(\nu'_{kL})^c\right.\\ &\left.+(U_R^\nu)_{bk}\nu'_{kR}\right)H_5^-\\ &+\frac{h_{ab}^\nu\omega}{\sqrt{u^2+\omega^2}}\overline{(N'_{jR})^c}(U_R^{N*})_{ja}\\ &\times\left((V^{\nu T})_{bk}(\nu'_{kL})^c + (U_R^\nu)_{bk}\nu'_{kR}\right)H'_o + H.c.\end{aligned}$$

The charged currents associated with the new gauge bosons are written in the physical states as follows

$$\begin{aligned}\mathcal{L}_{W,Y}^{\mathrm{lepton}} &= -\frac{g}{\sqrt{2}}\left\{\bar{\nu}_{aL}\gamma^\mu e_{aL}W_\mu^+ + \bar{e}_{aL}\gamma^\mu(N_{aR})^c Y_\mu^-\right\} + H.c.\\ &= -\frac{g}{\sqrt{2}}\left\{\left(\bar{\nu}'_{kL}(U_L^{\nu*})_{ka} + \overline{(\nu'_{kR})^c}V_{ka}^{\nu*}\right)\gamma^\mu(U_L^l)_{aj}e'_{jL}W_\mu^+\right.\\ &\left.+\bar{e}'_{kL}(U_L^{l*})_{ka}\gamma^\mu(U_R^{N*})_{aj}(N'_{jR})^c Y_\mu^-\right\} + H.c..\end{aligned} \quad (65)$$

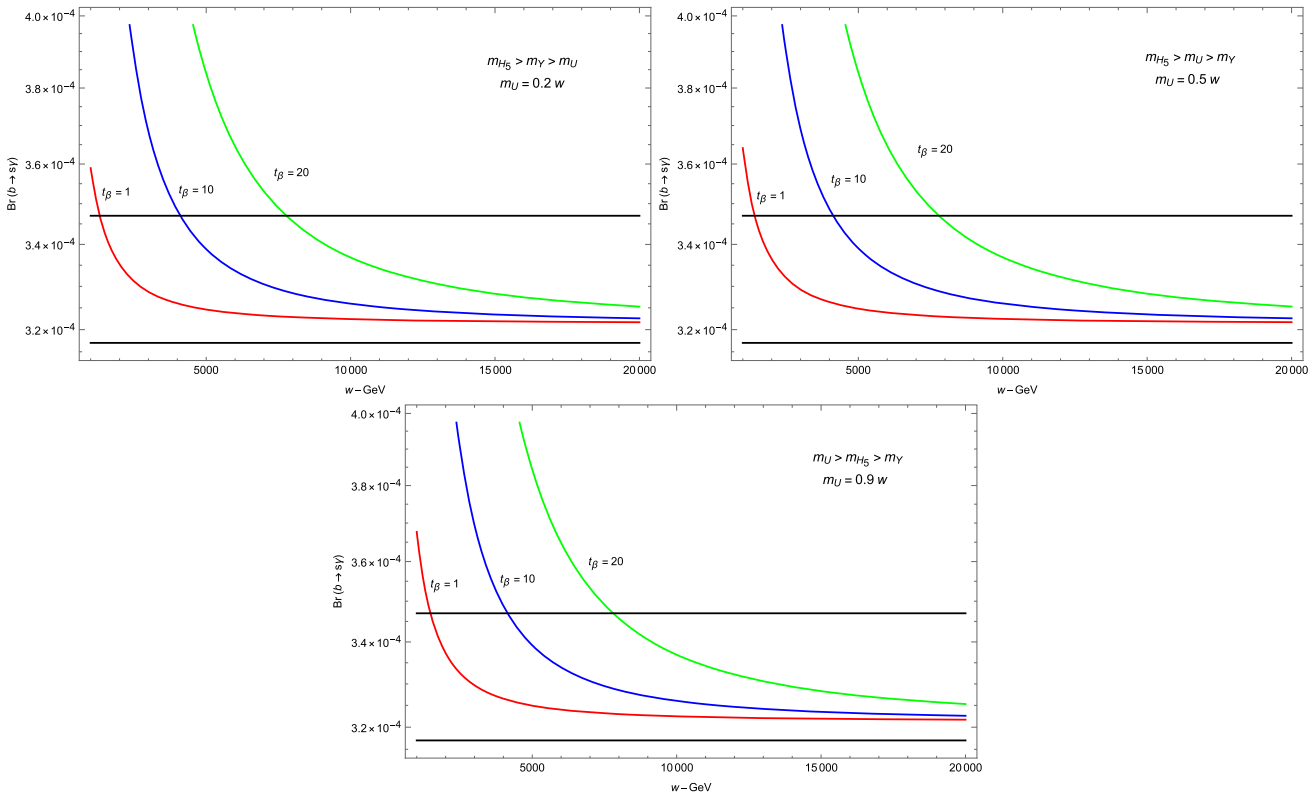

Fig. 4 The dependence of the Br$(b \to s\gamma)$ on the NP scale w in the limit, $u, v \ll -f\frac{u^2+v^2}{uv} \sim w \sim \Lambda$. The solid black lines indicate the current experimental constraint Br$(b \to s\gamma) = (3.32 \pm 0.15) \times 10^{-4}$ [39]

Next, we write the effective Lagrangian relevant for the $\mu \to e\gamma$ processes in the traditional form

$$\mathcal{L}_{\text{eff}}^{\mu\to e\gamma} = -4\frac{eG_F}{\sqrt{2}} m_\mu \left(A_R \bar{e}\sigma_{\mu\nu} P_R \mu + A_L \bar{e}\sigma_{\mu\nu} P_L \mu\right) F^{\mu\nu} + H.c., \tag{66}$$

where the factors A_L, A_R are obtained by calculating all the one-loop diagrams. We use the 't Hooft–Feynman gauge and keep the external lepton masses for calculations. The obtained results are inspired by [66]. The factors $A_{L,R}$ are divided into individual contributions, as shown below

$$A_{L,R} = A_{L,R}^W + A_{L,R}^Y + A_{L,R}^{H_5} + A_{L,R}^{H_4}, \tag{67}$$

where

$$A_R^W = -\frac{eg^2}{32\pi^2 m_W^2}\sum_{j=1}^{3}(U_L^{\nu *})_{\mu j}(U_L^{\nu})_{ej} f\left(\frac{m_{\nu_j}^2}{m_W^2}\right),$$

$$A_L^W = -\frac{eg^2 m_e}{32\pi^2 m_W^2 m_\mu}\sum_{j=1}^{3}(U_L^{\nu *})_{\mu j}(U_L^{\nu})_{ej} f\left(\frac{m_{\nu_j}^2}{m_W^2}\right),$$

$$A_R^Y = -\frac{eg^2}{32\pi^2 m_Y^2}\sum_{j=1}^{3}(U_R^{N *})_{\mu j}(U_R^{N})_{ej} f\left(\frac{m_{N_j}^2}{m_Y^2}\right),$$

$$A_L^Y = -\frac{eg^2 m_e}{32\pi^2 m_Y^2 m_\mu}\sum_{j=1}^{3}(U_R^{N *})_{\mu j}(U_R^{N})_{ej} f\left(\frac{m_{N_j}^2}{m_Y^2}\right),$$

$$A_L^{H_5} = -\frac{eg^2 m_e m_\mu}{32\pi^2 m_W^2 m_{H_5}^2 t_\beta^2}\sum_{j=1}^{3}(U_L^{\nu *})_{\mu j}(U_L^{\nu})_{ej} g\left(\frac{m_{\nu_j}^2}{m_{H_5}^2}\right) - \frac{eg^2 m_e v^2}{64\pi^2 m_W^2 m_{H_5}^2 m_\mu}\sum_{j,k=1}^{3}(h^{\nu *})_{\mu j}(h^{\nu})_{ej}(U_R^{\nu})_{jk} \times (U_R^{\nu *})_{jk} g\left(\frac{M_{\nu_j}^2}{m_{H_5}^2}\right) - \frac{eg^2 v^2 m_e}{64\pi^2 m_W^2 m_{H_5}^2 m_\mu}\sum_{j,k=1}^{3}(h^{\nu *})_{\mu j}(h^{\nu})_{ej} \times (V^{\nu T})_{jk}(V^{\nu T *})_{jk} g\left(\frac{M_{\nu_j}^2}{m_{H_5}^2}\right),$$

$$A_R^{H_5} = -\frac{eg^2 m_e^2}{32\pi^2 m_W^2 m_{H_5}^2 t_\beta^2}\sum_{j=1}^{3}(U_L^{\nu *})_{\mu j}(U_L^{\nu})_{ej} g\left(\frac{m_{\nu_j}^2}{m_{H_5}^2}\right) - \frac{eg^2 v^2}{64\pi^2 m_W^2 m_{H_5}^2}\sum_{j,k=1}^{3}(h^{\nu *})_{\mu j}(h^{\nu})_{ej}(U_R^{\nu})_{jk} \times (U_R^{\nu *})_{jk} g\left(\frac{M_{\nu_j}^2}{m_{H_5}^2}\right)$$

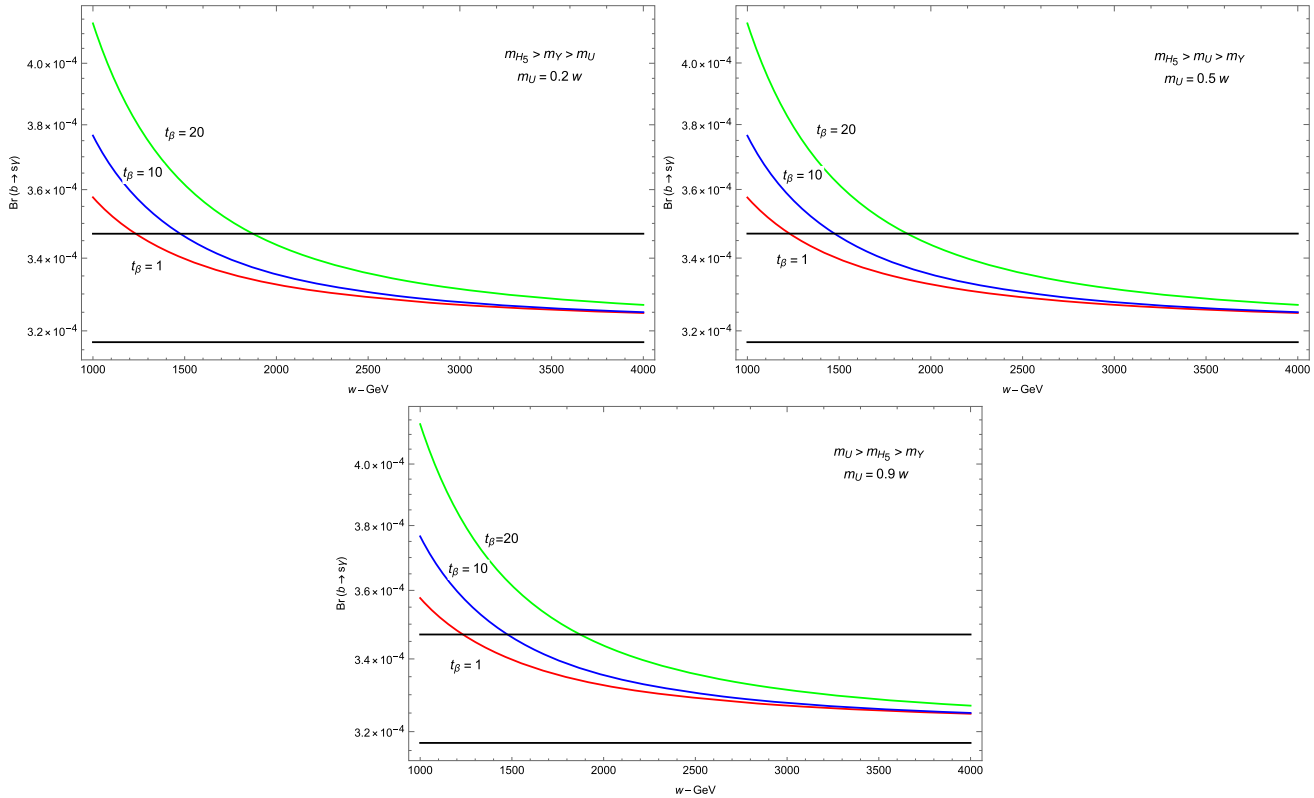

Fig. 5 The dependence of the branching ratio $\mathrm{Br}(b \to s\gamma)$ on the NP scale w in the limit $u, v \ll -f \sim w \sim \Lambda$. The solid black lines indicate the current experimental constraint $\mathrm{Br}(b \to s\gamma) = (3.32 \pm 0.15) \times 10^{-4}$ [39]

$$
\begin{aligned}
&-\frac{eg^2v^2}{64\pi^2 m_W^2 m_{H_5}^2}\sum_{j,k=1}^{3}(h^{\nu *})_{\mu j}(h^{\nu})_{ej}(V^{\nu T})_{jk}\\
&\times(V^{\nu T *})_{jk}\,g\left(\frac{M_{\nu_j}^2}{m_{H_5}^2}\right),\\
A_L^{H_4} &= -\frac{eg^2 m_e m_\mu}{32\pi^2 m_Y^2 m_{H_4}^2 t_{\beta'}^2}\sum_{j=1}^{3}(U_R^{N*})_{\mu j}(U_R^N)_{ej}\,g\left(\frac{m_{N_j}^2}{m_{H_4}^2}\right),\\
A_R^{H_4} &= -\frac{eg^2 m_e^2}{32\pi^2 m_Y^2 m_{H_4}^2 t_{\beta'}^2}\sum_{j=1}^{3}(U_R^{N*})_{\mu j}(U_R^N)_{ej}\,g\left(\frac{m_{N_j}^2}{m_{H_4}^2}\right),
\end{aligned}
\tag{68}
$$

The functions $f(x)$ and $g(x)$ are defined by

$$
\begin{aligned}
f(x) &= \frac{10 - 43x + 78x^2 - 48x^3 + 4x^4 + 18x^3\log x}{12(x-1)^4},\\
g(x) &= \frac{1 - 6x + 3x^2 + 2x^3 - 6x^2\log x}{12(x-1)^4}.
\end{aligned}
\tag{69}
$$

The notations $m_{\nu_j}, M_{\nu_j}, m_e, m_\mu$ are understood as the masses of light, heavy neutrinos, electron, and muon, respectively.

From the effective Lagrangian (66), we finally got the branching ratio $\mathrm{Br}(\mu \to e\gamma)$ as follows

$$
\mathrm{Br}(\mu \to e\gamma) = \frac{12\pi^2}{G_F^2}(|A_L|^2 + |A_R|^2)\mathrm{Br}(\mu \to e\tilde{\nu_e}\nu_\mu),
\tag{70}
$$

where $G_F = \frac{g^2}{4\sqrt{2}m_W^2}$ is the Fermi coupling constant, $\mathrm{Br}(\mu \to e\tilde{\nu_e}\nu_\mu) = 100\%$ as given in [40].

Before considering numerical calculations of the branching ratio $\mathrm{Br}(\mu \to e\gamma)$, let us make some assumptions. We assume that a diagonal matrix presents the Yukawa couplings h_{ab}^e in the flavor basis. Thus, the matrix U_L^ν is identified as the PMNS matrix U_{PMNS}, which has been measured experimentally. Both the mixing matrices U_R^ν, V^ν as well as $U_{L,R}^N$ are new and not constrained by experiments. To simplify, we suppose that the Yukawa couplings of the right-handed neutrinos h'^ν are presented by a diagonal matrix. This indicates that the Majorana neutrino mass matrix has the form as $M_R^\nu = \mathrm{Diag}(M_{\nu_1}, M_{\nu_2}, M_{\nu_3})$ and thus the right-handed neutrino mixing mass matrix U_R^ν is a unit matrix. The mixing matrix V^ν is also assumed to be diagonal. Finally, for the mixing matrix of the new leptons U_R^N, we can use three arbitrary angles θ_{ij}^N, $(i, j = 1, 2, 3)$ and a Dirac CP phase δ^N to parameterize.

With the above option, the Yukawa couplings h^e, h'^ν can be translated into the charged lepton and sterile neutrino masses as follows

$$h^e = -\frac{\sqrt{2}}{v}\text{Diag}\left(m_e, m_\mu, m_\tau\right),$$
$$h'^\nu = -\frac{1}{\sqrt{2}\Lambda}\text{Diag}\left(M_{\nu_1}, M_{\nu_2}, M_{\nu_3}\right). \quad (71)$$

The Yukawa couplings h^ν, which determine the neutrino Dirac mass, are rewritten by using Casas-Ibarra parametrization as given in [65]

$$h^\nu = \frac{\sqrt{2}}{u}\begin{pmatrix}\sqrt{M_{\nu_1}} & 0 & 0\\ 0 & \sqrt{M_{\nu_2}} & 0\\ 0 & 0 & \sqrt{M_{\nu_3}}\end{pmatrix} R \begin{pmatrix}\sqrt{m_{\nu_1}} & 0 & 0\\ 0 & \sqrt{m_{\nu_2}} & 0\\ 0 & 0 & \sqrt{m_{\nu_3}}\end{pmatrix} U_L^{\nu\dagger}, \quad (72)$$

where R is an orthogonal matrix which is presented via arbitrary angles as the following

$$R = \begin{pmatrix}\hat{c}_2\hat{c}_3 & -\hat{c}_1\hat{s}_3 - \hat{s}_1\hat{s}_2\hat{c}_3 & \hat{s}_1\hat{s}_3 - \hat{c}_1\hat{s}_2\hat{c}_3\\ \hat{c}_2\hat{s}_3 & \hat{c}_1\hat{c}_3 - \hat{s}_1\hat{s}_2\hat{s}_3 & -\hat{s}_1\hat{c}_3 - \hat{c}_1\hat{s}_2\hat{s}_3\\ \hat{s}_2 & \hat{s}_1\hat{c}_2 & \hat{s}_1\hat{c}_2\end{pmatrix} \quad (73)$$

with $\hat{s}_i = \sin\hat{\theta}_i, \hat{c}_i = \cos\hat{\theta}_i, i = 1, 2, 3$ and $\hat{\theta}_{ij} \in [0, \pi/2]$.

For the magnitudes of relevant masses and the VEVs, we also work on the limits $u, v \ll w \sim \Lambda$, $u^2 + v^2 = 246^2$ GeV^2. To be consistent with the unitary bound [67], we need the constraint: $m_N < 16 m_Y$. The masses of new charged Higgs $H^\pm_{4,5}$ and new gauge boson $Y^\pm$ are approximately taken as similar in the Sect. 4.1. In keeping with constraints from dark matter studies in [32], the new fermion mass is at the TeV scale. The mixing angle $t_{\beta'}$ can be expressed via the energy scales u, w such as $t_{\beta'} = \sqrt{246^2 - u^2}/w$. Other known parameters are taken from [40] as given

$$\begin{aligned} m_W &= 80.385\ \text{GeV}, \quad m_e = 0.5109989461\ \text{MeV},\\ m_\mu &= 105.6583745\ \text{MeV},\\ \sin^2(\theta_{12}) &= 0.307, \quad \sin^2(\theta_{23}) = 0.51,\\ \sin^2(\theta_{13}) &= 0.021, \quad \alpha = \frac{1}{137},\\ \Delta m^2_{12} &= 7.53\times 10^{-5}\ \text{eV}^2, \quad \Delta m^2_{23} = 2.45\times 10^{-3}\ \text{eV}^2, \end{aligned} \quad (74)$$

where θ_{ij} are the mixing angles of the neutrino mixing matrix.

In addition, the branching ratio $\text{Br}(\mu \to e\gamma)$ also depends on the unknown parameters, such as six mixing angles ($\hat{\theta}_{ij}$, θ^N_{ij}), one CP phase δ^N, the masses of new particles m_N, M_{ν_i}. In the following, we are going to present the results of numerical calculations for the case where unknown parameters are chosen as

$$\begin{aligned} \theta^N_{12} &= \pi/6, \quad \theta^N_{13} = \pi/3,\\ \theta^N_{23} &= \pi/4, \quad \delta^N = 0, \end{aligned}$$

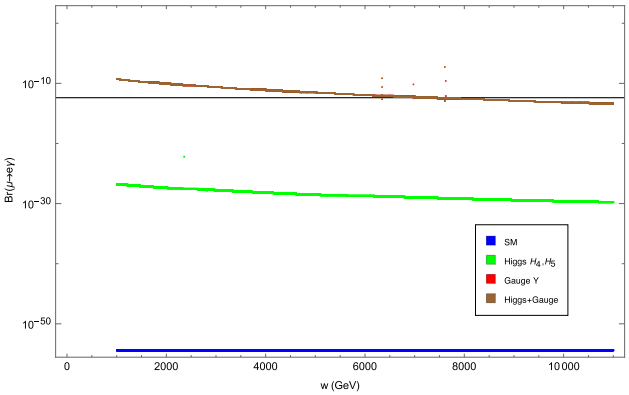

Fig. 6 The figure presents the dependence of the branching ratio $\text{Br}(\mu \to e\gamma)$ on the NP scale w for each contribution. The solid black line indicates the upper from the experiment [40]. Here $u = 10$ GeV

$$\begin{aligned} \hat{\theta}_1 &= \pi/3, \quad \hat{\theta}_2 = \pi/4,\\ \hat{\theta}_3 &= \pi/6,\\ m_{\nu_1} &= 0.01\ \text{eV}, \quad M_{\nu_1} = 10^9\ \text{GeV},\\ M_{\nu_2} &= M_{\nu_3} = 10^3 M_{\nu_1},\\ m_{N_1} &= 2000\ \text{GeV}, \quad m_{N_2} = 2200\ \text{GeV},\\ m_{N_3} &= 2400\ \text{GeV}. \end{aligned} \quad (75)$$

The Fig. 6 estimates the value of each contribution into the $\text{Br}(\mu \to e\gamma)$. The dominant contribution comes from the new gauge bosons $Y^\pm$. The NP scale is strongly constrained by the experiments [40], $\text{Br}(\mu \to e\gamma)_{\text{exp}} < 4.2\times 10^{-13}$. To be consistent with this bound, the NP scale satisfies $w > 7.3$ TeV, which is similar to the bound derived from studying the $b \to s\gamma$ decay.

The Fig. 7 demonstrates $\text{Br}(\mu \to e\gamma)_{\text{total}}$ as a function of NP scale w with three different values of the electroweak scale, u, $u = 5$ GeV, $u = 10$ GeV and $u = 20$ GeV. There is no separation between the graphs corresponding to different choices of u. As a result, the $\text{Br}(\mu \to e\gamma)_{\text{total}}$ depends very weakly on the u. It is important to keep in mind that the factors $A^{H_4,H_5}_{L,R}$ are greatly influenced by the electroweak scales u and v. Therefore, this result shows that the charged currents associated with the charged Higgs particles have negligible influence on the $\mu \to e\gamma$ decay and may be ignored. Strong constraints are imposed on the charged current associated with new gauge bosons.

5 Conclusions

In the 3-3-1-1 model, the tree-level FCNCs appear due to the non-universal assignment of quark families. Experiments on meson oscillations strongly constrain these interactions. We computed the mass difference for $K^0 - \bar{K}^0$, $B^0_d - \bar{B}^0_d$, $B^0_s - \bar{B}^0_s$ based on the tree-level FCNCs and noticed that the main

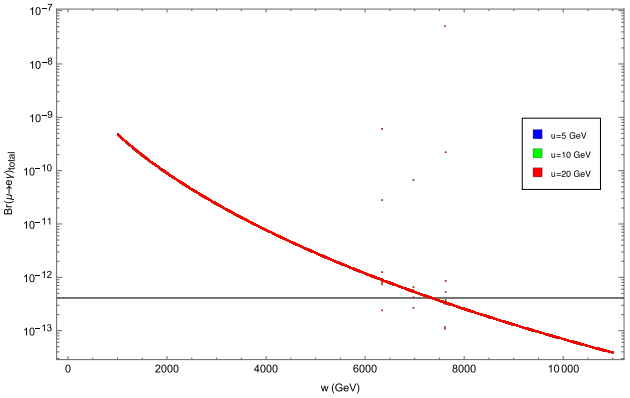

Fig. 7 The figure presents the comparison of the dependence of the total branching ratio $\mathrm{Br}(\mu \to e\gamma)_{\mathrm{total}}$ on the NP scale w with $u = 5$ GeV, $u = 10$ GeV and $u = 20$ GeV, respectively. The solid black line indicates the upper bound from the experiment [40]

contributions to the meson oscillations come from the new neutral gauge bosons mediation. The NP scale is strongly constrained by the experimental bounds on mixing mass parameters. We have obtained the lower bound on the new gauge boson mass $\mathrm{M_{new}} > 12$ TeV, which is more stringent than the constraint previously given in [32]. This change is because previous studies omitted the contributions of new Higgs, especially those of the SM. Our result is consistent with that of [68]. We also studied the tree-level FCNCs affecting the branching ratio of $B_s \to \mu^+\mu^-$, $B \to K^*\mu^+\mu^-$ and $B^+ \to K^+\mu^+\mu^-$. In the parameter region consistent with the experimental constraints on the meson mass difference, the tree-level FCNCs give small contributions to these branching ratios, which is consistent with the measurement $B_s \to \mu^+\mu^-$ [4–7] but can not explain the $B \to K^*\mu^+\mu^-$ and $B^+ \to K^+\mu^+\mu^-$ anomalies [16–24].

For the radiative decay processes, we concentrated on the flavor-changing $b \to s\gamma$ decay. The large contribution arises from the Wilson coefficient $C_7^{H_5}$ yielded from one-loop diagrams with the new charged Higgs boson mediation. In spite of the enhanced contributions due to the factor $t_\beta = v/u$, the predicted branching ratio $\mathrm{Br}(b \to s\gamma)$ is consistent with the measurement [39], if $\mathrm{M_{new}}$ is chosen as above mentioned. In contrast to the $b \to s\gamma$ decay, the branching ratio of the lepton flavor-violating $\mu \to e\gamma$ decay obtains a large contribution from one-loop diagrams with new gauge bosons exchange. Due to the large mixing of new neutral leptons, the branching ratio $\mathrm{Br}(\mu \to e\gamma)$ can reach the experimental upper bound.

Acknowledgements This research is funded by the Vietnam National Foundation for Science and Technology Development (NAFOSTED) under Grant Number 103.01-2019.312.

Data Availability Statement My manuscript has associated data in a data repository. [Authors' comment: There is no experimental data because this is a theoretical study.]

Funded by SCOAP[3].

References

1. V.M. Abazov et al. (DØcollaboration), Phys. Rev. D **97**, 112002 (2006)
2. A. Abulencia et al. (CDF collaboration), Phys. Rev. Lett. **97**, 062003 (2006)
3. V.M. Abazov et al. (DØcollaboration), Phys. Rev. Lett. **97**, 021802 (2006)
4. V. Khachatryan et al. (CMS and LHCb Collaborations), Nature **522**, 68 (2015)
5. R. Aaij et al. (LHCb Collaboration), Phys. Rev. Lett. **108**, 231801 (2012)
6. R. Aaij et al. (LHCb Collaboration), Phys. Rev. Lett. **110**, 021801 (2013)
7. M. Santimaria (LHCb Collaboration), LHC Seminar "New results on theoretically clean observables in rare B-meson decays from LHCb", 23 March (2021). https://indico.cern.ch/event/976688/attachments/2213706/3747159/santimaria_LHC_seminar_2021.pdf
8. R. Ammar et al. (CLEO Collaboration), Phys. Rev. Lett. **71**, 674 (1993)
9. R. Barate et al. (ALEPH Collaboration), Phys. Lett. B **429**, 169 (1998)
10. S. Chen et al. (CLEO Collaboration), Phys. Rev. Lett. **87**, 251807 (2001)
11. B. Aubert et al. (BABAR Collaboration), arXiv:hep-ex/0207074. arXiv:hep-ex/0207076
12. R. Aaij et al. (LHCb Collaboration), JHEP **08**, 55 (2017)
13. S. Wehle et al. (Belle Collaboration), Phys. Rev. Lett. **126**, 161801 (2021)
14. R. Aaij et al. (LHCb Collaboration), Phys. Rev. Lett. **113**, 151601 (2014)
15. R. Aaij et al. (LHCb Collaboration), Phys. Rev. Lett. **122**, 191801 (2019)
16. R. Aaij et al. (LHCb Collaboration), Phys. Rev. Lett. **126**, 161802 (2021)
17. R. Aaij et al. (LHCb Collaboration), JHEP **04**, 064 (2015)
18. Khachatryan et al. (CMS Collaboration), Phys. Lett. B **753**, 424 (2016)
19. S. Wehle et al. (Belle Collaboration), Phys. Rev. Lett. **118**, 111801 (2017)
20. A.M. Sirunyan et al. (CMS Collaboration), Phys. Rev. D **98**, 112011 (2018)
21. M. Aaboud et al. (ATLAS Collaboration), JHEP **10**, 047 (2018)
22. R. Aaij et al. (LHCb Collaboration), Phys. Rev. Lett. **125**, 011802 (2020)
23. R. Aaij et al. (LHCb Collaboration), Eur. Phys. J. C **77**, 161 (2017)
24. R. Aaij et al. (LHCb Collaboration), JHEP **06**, 133 (2014)
25. F. Pisano, V. Pleitez, Phys. Rev. D **46**, 410 (1992)

26. P.H. Frampton, Phys. Rev. Lett. **69**, 2889 (1992)
27. R. Foot, O.F. Hernandez, F. Pisano, V. Pleitez, Phys. Rev. D **47**, 4158 (1993)
28. M. Singer, J.W.F. Valle, J. Schechter, Phys. Rev. D **22**, 738 (1980)
29. J.C. Montero, F. Pisano, V. Pleitez, Phys. Rev. D **47**, 2918 (1993)
30. R. Foot, H.N. Long, T.A. Tran, Phys. Rev. D **50**, R34 (1994)
31. P.V. Dong, T.D. Tham, H.T. Hung, Phys. Rev. D **87**, 115003 (2013)
32. P.V. Dong, D.T. Huong, F.S. Queiroz, N.T. Thuy, Phys. Rev. D **90**, 075021 (2014)
33. D.T. Huong, P.V. Dong, C.S. Kim, N.T. Thuy, Phys. Rev. D **91**, 055023 (2015)
34. D.T. Huong, P.V. Dong, Eur. Phys. J. C **77**, 204 (2017)
35. P.. V.. Dong, D.. T. Huong, Daniel A. Camargo, Farinaldo S. Queiroz, José W. F.. Valle, Phys. Rev. D **99**, 055040 (2019)
36. P.V. Dong, D.T. Si, Phys. Rev. D **93**, 115003 (2016)
37. T. Jubb et al., Nucl. Phys. B **915**, 431 (2017)
38. A.J. Buras, F.D. Fazio, JHEP **08**, 115 (2016)
39. Y.S. Amhis et al. (HFLAV), Eur. Phys. J. C **81**, 226 (2021)
40. P.A. Zyla et al. (Particle Data Group), Prog. Theor. Exp. Phys. **083C01** (2020)
41. C.W. Chiang, X.G. He, J. Tandean, X.B. Yuan, Phys. Rev. D **96**, 115022 (2017)
42. P. Gambino, K.J. Healey, S. Turczyk, Phys. Lett. B **763**, 60–65 (2016)
43. J. Charles et al., Phys. Rev. D **91**, 073007 (2015)
44. M. Bona (UTfit Collaboration), PoS **ICHEP2016**, 554 (2016)
45. S. Aoki et al. (Flavour Lattice Averaging Group), Eur. Phys. J. C **80**, 113 (2020)
46. M. Beneke, C. Bobeth, R. Szafron, Phys. Rev. Lett. **120**, 011801 (2018)
47. K. De Bruyn, R. Fleischer, R. Knegjens, P. Koppenburg, M. Merk, N. Tuning, Phys. Rev. D **86**, 014027 (2012)
48. C. Bobeth, M. Gorbahn, T. Hermann, M. Misiak, E. Stamou, M. Steinhauser, Phys. Rev. Lett. **112**, 101801 (2014)
49. T. Aaltonen et al. (CDF Collaboration), Phys. Rev. Lett. **102**, 201801 (2009)
50. M. Beneke, C. Bobeth, R. Szafron, JHEP **10**, 232 (2019)
51. S. Descotes-Genon, L. Hofer, J. Matias, J. Virto, JHEP **06**, 092 (2016)
52. S. Descotes-Genon, J. Matias, J. Virto, Phys. Rev. D **88**, 074002 (2013)
53. A.K. Alok, A. Dighe, S. Gangal, D. Kumar, JHEP **06**, 089 (2019)
54. M. Algueró, B. Capdevila, S. Descotes-Genon, J. Matias, M. Novoa-Brunet, arXiv:2104.08921 [hep-ph]
55. L.S. Geng, B. Grinstein, S. Jäger, S.Y. Li, J. Martin Camalich, R.X. Shi, arXiv:2103.12738 [hep-ph]
56. W. Altmannshofer, P. Stangl, arXiv:2103.13370 [hep-ph]
57. T. Hurth, F. Mahmoudi, S. Neshatpour, Phys. Rev. D **103**, 095020 (2021)
58. C. Cornella, D.A. Faroughy, J. Fuentes-Martín, G. Isidori, M. Neubert, arXiv:2103.16558 [hep-ph]
59. M. Misiak et al., Phys. Rev. Lett. **114**, 221801 (2015)
60. M. Czakon et al., JHEP **04**, 168 (2015)
61. T. Inami, C.S. Lim, Prog. Theor. Phys **65**, 297 (1981)
62. M. Misiak, M. Steinhauser, Nucl. Phys. B **764**, 62–82 (2007)
63. A.J. Buras, F.D. Fazio, J. Girrbach, M.V. Carlucci, JHEP **02**, 23 (2013)
64. A.J. Buras, L. Merlo, E. Stamou, JHEP **08**, 124 (2011)
65. J.A. Casas, A. Ibarra, Nucl. Phys. B **618**, 171 (2001)
66. L. Lavoura, Eur. Phys. J. C **29**, 191 (2003)
67. M.S. Chanowitz, M.A. Furman, I. Hinchliffe, Phys. Lett. B **78**, 285 (1978)
68. R.H. Benavides, Y. Giraldo, W.A. Ponce, Phys. Rev. D. **80**, 113009 (2009)